p. 48

UNC CHARLOTTE

MAGNETOSTRICTIVE DIRECT DRIVE MOTORS

By

Dipak Naik

P.H. DeHoff, P.I.

Final Report

June 30, 1992

NASA Grant NAG 5-1169

Technical Report ME & ES 92-2
Department of Mechanical Engineering & Engineering Science

University of North Carolina at Charlotte

Charlotte, NC 28223

ABSTRACT

A new rare-earth alloy Terfenol-D combines low frequency operation and extremely high energy density with high magnetostriction. Its material properties make it suitable as a drive element for actuators requiring high output torque. The high strains, the high forces and the high controllability of Terfenol alloys provide a powerful and challenging basis for new ways to generate motion in actuators.

Two prototypes of motors utilizing Terfenol-D rods have been developed at NASA, Goddard Space Flight Center. Section I of this report provides the basic principles of operation of the motor and other relevant details. A conceptual design of a torque limiting safety clutch/brake under development is illustrated in Section II. Section III shows preliminary design drawings of a linear actuator utilizing Terfenol-D.

Section I
Magnetostrictive Rotary Motors

The details of the direct drive rotary motor were presented at the International Magnetics Conference in St. Louis, MO on April 13-16, 1992. Co-authors of this paper, along with Dr. D.P. Naik were John Vranish of NASA Goddard Space Flight Center, J.P. Teter and J.B. Restoff of the Naval Surface Warfare Center. A companion paper was published in the IEEE Transactions on Magnetics, Vol 27, No 6 in November, 1991. A reprint of the conference presentation is reproduced in the following section.

MAGNETOSTRICTIVE DIRECT DRIVE REVERSIBLE ROTARY MOTORS

J.P. Teter and J.B. Restorff
R43, Naval Surface Warfare Center,
Silver Spring, MD 20903-5000

D.P. Naik and J.M. Vranish
NASA Goddard Space Flight Center,
Greenbelt, MD 20771

Abstract----Highly magnetostrictive materials such as $Tb_{.3}Dy_{.7}Fe_2$, commercially known as TERFENOL-D, have been used to date in a variety of devices such as high power actuators and linear motors. The larger magnetostriction available in twinned single crystal TERFENOL-D, approximately 2000 ppm at moderate magnetic field strengths, makes possible a new generation of magneto-mechanical devices. The authors are investigating the potential of this material as the basis of a direct micro-stepping rotary motor with torque densities on the order of industrial hydraulics and five times greater than that of the most efficient, high power electric motors. Such a motor would be a micro-radian stepper, capable of precision movements and self-braking in the power off state. Two motor prototypes are being developed and competed against each other, one based on the proven "Inch Worm" technique and the other based on entirely new "Roller Locking" principle which eliminates pounding and the need for active clamping.

The thrust of this paper is to juxtapose innovative mechanical engineering techniques on proper magnetic circuit design to reduce losses in structural flexures, inertias, thermal expansions, eddy currents and magneto-mechanical coupling, thus optimizing motor performance and efficiency. Mathematical modelling techniques will be presented, to include magnetic, structural and both linear and non-linear dynamic calculations. In addition, test results on prototype hardware will be presented, including some promising early results.

I. INTRODUCTION

The performance of robots in space will ultimately be limited by the motors which drive them. These electromagnetic motors are limited in their torque density, hence they depend on high speed to generate power. This means that they must derive torque and force multiplication through gear reduction systems. And this in turn, means that the size of the motor/drive system must grow and that the efficiency and reliability of the system as a whole must decrease. Also, since most high performance electromagnetic motors today are servo type and not steppers, they must either use brakes or must keep the power on the hold position. This serves to reduce the duty cycle, reduce system efficiency and create heat. It also leads to limit cycling. On the other hand, adding a brake also increases size and complexity and reduces reliability. And, even if current stepping motors could be brought up to performance standards of servo motors we would still have the problem of needing gear reduction and a brake (because the magnetic holding force is too weak to ensure adequate safety margins with the power off. An entirely new approach, the magnetostrictive direct drive motor is needed to redress the inadequacies described above.

Magnetostriction may provide a means of developing an electric motor with power densities on the order of industrial hydraulics (> 5 times present electric motors) and with a frequency response in the sonar range (6 KHz per cm of length). The magnetostrictive motors would be inherently self braking with the power off thus power, efficiency and safety would be improved. In addition to their space applications, such motors/actuators would have major spin-offs into the commercial and industrial sectors.

Several concepts based on magnetostrictive drives have been attempted, all with varying degrees of success. In this paper two distinctly different approaches, one using magnetostrictive drive and clamping rods (inch worm principle:prototype A) and one using magnetostrictive drive rods and a roller locking system for clamping (prototype B) are described.

II. LITERATURE REVIEW

Several magnetostrictive devices have been developed, most of which are linear motors. Linear motors operate on the "Inch Worm" principle such as is described in [1-8]. The motion generated in these devices is limited because of the nature of the materials typically used, (magnetostrictive or electrostrictive), the length of the translator and because electrical power must be provided to the active (and moving) portion of these motors. The Harvard motor described in reference [3] is rotary motor. However the principle used does not appear to lend itself to being developed into a practical motor due to several inherent disadvantages. First, the device is too bulky and the inertia of the rocker and the distance it must travel is a limiting factor on speed. Second, the force and torque are reduced because standard magnetic attraction techniques are used to power the device and the advantages of magnetostriction are used only in clamping. The ultrasonic motor illustrated in [4] is a magnetostrictive adaptation of the family of piezoelectric ultrasonic motors developed by Panasonic as described in reference [5]. This type of motor is limited in its torque output because the coupling between the elastic body and the rotating body is ultimately a frictional one. It is most appropriate as a piezoelectric system which places a premium on compactness and simplicity and in which torque can be modest. It is not particularly compact when magnetostrictive rods are used and as stated before, its torque capability is limited.

A. Disadvantages of Prior Art

Although Inch Worm technique is straight forward and proven it has several disadvantages. The "Inch Worm" technique has excessive coil losses because it requires dedicated active magnetostrictive elements to clamp. It also has critical tolerances on the clamping elements and it is difficult to get the clamping elements to adjust for wear without a prohibitive sacrifice in torque output. It is difficult to prevent large losses of torque and travel due to structural deflections. Also a lot of magnetostrictive

material is required, some for the drive elements and some for the clamping elements. And, the system is bulky because of the excessive number of active elements, the coil windings which go with them and the magnetic shielding required to keep the fields of each element from interfering with each other.

The "Kiesewetter" technique [2] is prone to excessive wear. Since it depends on an interference fit, this device will not retain its clamping power as it wears out. The large number of drive coils makes the electronics extremely complex as it must excite these coils, one by one. Thus the task of making a rotary motor based on this principle is formidable. Although the forces generated through this motor are large, the speed is low as linear stroke is limited.

The "Ultrasonic Motor" is torque limited because it has a frictional coupling between the elastic body and the drive. Also, it requires a number of magnetostrictive elements. While it is compact as a piezoelectric motor, that advantage is lost when magnetostrictive elements are used. All-in-all, it seems most appropriate as a piezoelectric motor.

B. Motor Design Goals

Current robot motors are very high speed; but have weak torque compensated by using a transmission with extensive gearing. Since safety brakes are also required in these joints, these brakes must be located to act on the motor itself or the drive shaft on the motor side of the transmission to give them sufficient holding leverage. All these additions, compensations and restrictions lead to complications, lower reliability and controls problems. The magnetostrictive motor addresses these concerns by developing outstanding torque density and is self-braking with the power off. This permits the power to be taken directly off the drive shaft, eliminating brakes and transmissions. The magnetostrictive phenomenon using the material Terfenol-D shows promise because it generates impressive forces (> 28 MPa) and has excellent frequency response (6 KHz for 0.635 cms dia. rod). However, it also has three significant drawbacks, it has a very short stroke (0.001 cm/cm), low magnetic permeability (5) [8] and low magnetomechanical coupling coefficient of 0.7 resulting in fifty percent efficiency. These drawbacks present formidable engineering challenges. Power lost in heat reduces the current in the Terfenol coils and thus affects the Terfenol performance. Earlier attempts to design a magnetostrictive rotary motor have not been successful due to inherent properties of Terfenol-D. Small stroke limits the rotary speed of motor. The supporting structure has to be carefully designed as Terfenol rods are hard, brittle and sensitive to fracture and hence enable to withstand shear and bending loads. This requires precision mechanical engineering which had been lacking in earlier attempts to design the rotary motor. Following design goals are set forth for the rotary motor after giving due consideration to the requirements of space applications and inherent advantages offered by Terfenol-D.

- Direct drive/compact package-high torque density
- Fail safe holding torque self locking with power off
- Microradian-size steps leading to precision control
- No limit cycling
- Simple/reliable-minimal number of moving parts
- Outstanding agility-high frequency response

III. APPROACH

Two prototypes based on Inch Worm and Roller Locking principle respectively are designed and are enumerated as follow.

Inch Worm Principle

The motor incorporates mechanically prestressed Terfenol-D rods for clamping and driving the drive discs, permanent magnets for magnetic bias and magnetic fields generated by electrical coils. The Magnetostrictive motor has two important modules (Fig. 1), namely a pole pair and a drive element. Pole pair is essentially a clutch device and its function is to either lock or unlock drive disc. The top and bottom drive discs are splined to the shaft. Drive element, transfers a torque to output shaft through drive disc and a pole pair. A pole pair having 'C' shaped cross section holds a number of Terfenol rods. The top and bottom flanges of a pole pair has number of slots resulting into number of cantilevers. Each pair of cantilever is associated with a clamping Terfenol-D rod and serves the purpose of prestressing the Terfenol rods and allow the expansion of Terfenol rods under magnetic field. Mechanical compressive prestress is adopted to raise the magnetostriction of Terfenol and to keep the Terfenol rod from tensile stress condition because of its relative low tensile strength.

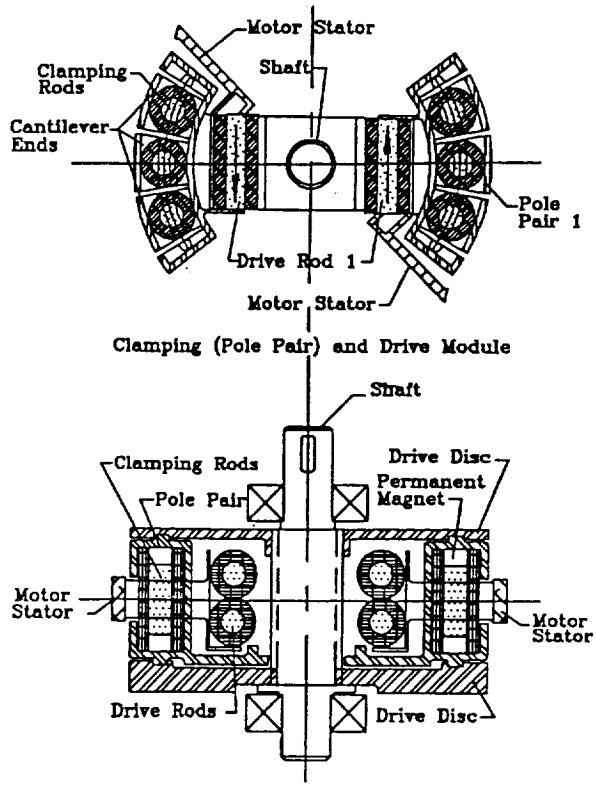

Fig. 1 Pole Pair and Drive Elements

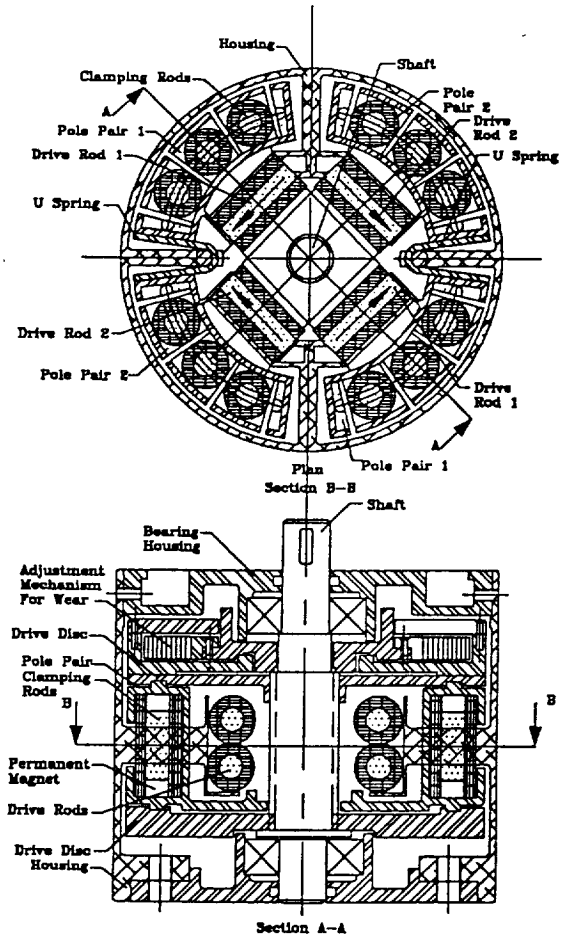

Fig. 2 Magnetostrictive Direct Drive Rotary Motor

When the Terfenol rods are energized through electric coils, they expand and deflect the cantilevered flange of the pole pair to make a firm contact with both the drive discs. Under no load condition this is achieved by the magnetic bias provided by the permanent magnets provided at the both the ends of the Terfenol rods. By adding permanent magnets to the pole pair the neutral position of the Terfenol rods can be shifted. Thus, when power is off, motor is self locked preventing any possibility of back driving under load. The self locking feature of this motor is attractive as it eliminates the additional device to lock the motor under no load, a requirement which renders conventional motor applications in space relatively costly as it limits the payload capacity of robots. Another advantage of the permanent magnetic bias field here is that now the maximum current needed in the coil is reduced by a factor of 2 and thus the coil losses by a factor of 4. The required current values can again be reduced by a factor of 2 by adding magnetic flux return to the pole pair design. This leads to decrease in a coil loss by a factor of 16 compared to the no permanent magnets, no magnetic flux return design.

The drive discs can be unlocked if needed by driving the Terfenol rod in opposite direction. Two such pole pairs in the form of 150^{o} circle sectors are used in this motor (Fig. 2). These pole pairs are coupled together by two 'U' springs and react against each other in a sequential manner.

The drive elements are enclosures for another set of Terfenol rods assembled in such a way that they are perpendicular to those in the pole pairs. Drive elements are mounted on stator (casing) of motor. The free ends of Terfenol rods rest on vertical flanges on pole pairs. Thus, when expanded they react against the pole pairs. Two such sets of rods react diametrically opposite against a pole pair simultaneously to generate a torque.

The basic principle of the Magnetostrictive motor is to mechanically clamp two parallel drive discs through a set of Terfenol rods in a pole pair. Driving the drive discs by two parallel sets of Terfenol rods in drive elements generate a torque acting in the plane parallel to that of the drive disc. The net result of this is to rotate the shaft through a step of the order of micro-radian. The Magnetostrictive motor incorporates two sets of pole pairs and two sets of drive elements which react against each other in a sequential manner to function as a micro-stepper motor. The cycle of events which control the motion of the motor is as shown in Fig. 3 and is as follows.

- Release all drives and clamp both the pole pairs
- Unclamp pole pair 1
- Drive both the drive elements. (this generates a positive motion through pole pair 2. Note that both the pole pairs compress the 'U springs storing part of the energy in springs.)
- Clamp pole pair 1 and unclamp pole pair 2.
- Release drive element 1. (this generates motion through pole pair 1 by releasing 'U' springs)
- Repeat this cycle.

The motor designed for 40.68 N.M of torque at 60 rpm is shown in Fig. 2.

A. Expected Performance

The performance of the motor can be evaluated by number of benchmarks like torque, speed, and wear etc.

1. Torque

The torque of the motor depends on various parameters such as torque arm, materials, number of Terfenol rods per pole pair etc. For a 0.635 cm diameter Terfenol rod, 4 per pole pair, the clamping torque is 54.24 N.M. The drive torque of each drive module is 46 N.m. The motor is expected to work without slip as the clamping torque is higher than the drive torque.

2. Frequency Response

The frequency response depends on the inertia torque caused by load acceleration or deceleration, the inertia of the load, the operating speed and the angle of acceleration. The pole pairs, clamping rods and associated windings contribute to the zero load inertia. The inertias of top and bottom drive discs and shaft together with the no load inertia determine the full load

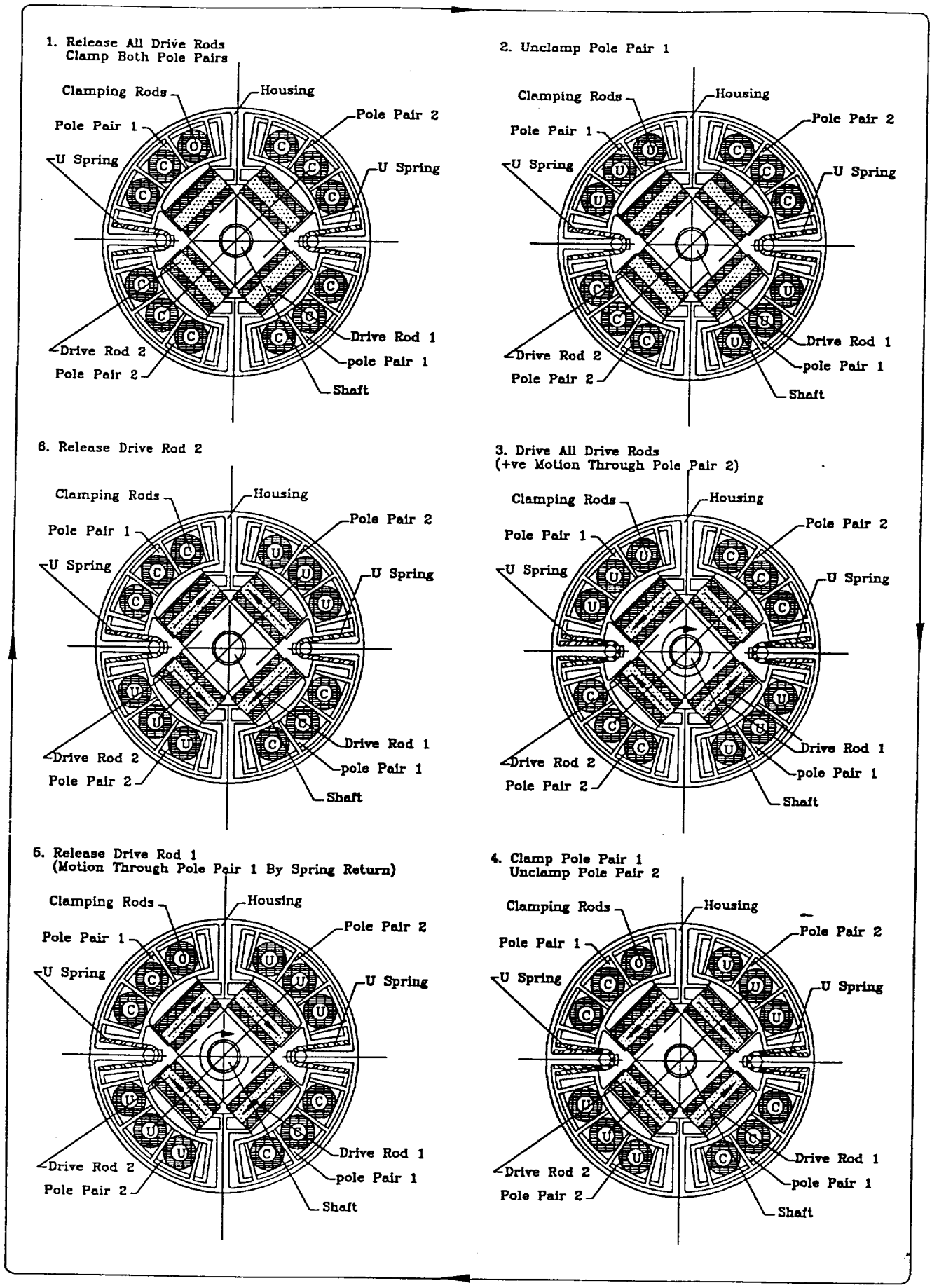

Fig. 3 Prototype 'A' Motion Cycle

frequency response of the motor. The results based on data taken from Fig. 2 is tabulated in the following table.

Table 1: No Load and Full Load Frequency Response of motor

Loading	Acceleration	Time	Frequency	RPM
	a (rad/sec^2)	t(sec.)	f_m (Hz)	n
No Load	27167.6	2.7E-4	3761.6	69
Full Load	20304.4	3.1E-4	3252.2	60

3. Deflections

The top and bottom drive discs are the only members susceptible to excessive deflections. However, the top drive disc is protected by a wear compensation mechanism. In view of this, the bottom drive disc is made heavier to withstand deflection. The deflection of the bottom drive disc should not exceed more than that of the expansion of the clamping rods. The deflection of the bottom drive disc is computed for the case of a flat circular disc fixed at the center and free at the outer rim [9] . The maximum calculated deflection of the bottom drive disc is 17.7 μ cms and is within permissible limits.

4. Wear

There are a large number of variables which affect wear. However, the most important ones are the load and the velocity, as these are dictated by the system requirements. The analytical technique for wear prediction is based on an engineering model for zero wear [10]. Zero wear is taken to be wear of such a magnitude that the surface finish in the wear track is not significantly different from the finish in the unworn portion. The condition for zero wear for N passes is given by following equation.

$$\gamma = \left(\frac{2*10^3}{N}\right)\gamma_R \qquad (1)$$

$$\tau_{max} = Kq_o\sqrt{(0.5)^2 + \mu^2} \qquad (2)$$

$$\gamma = \frac{\tau_{max}}{\tau_y} \qquad (3)$$

where,

$\gamma_R = 0.52$ and $K = 3$

μ = Coefficient of friction

q_o = Pressure between drive disc and top and bottom flanges

τ_{max} = Maximum shear stress

τ_y = Yield strength in shear

Evaluating the above equation for N we get N = 6.2 E17 passes. Adjustment for wear beyond this limit is taken care of by the adjustment mechanism for wear incorporated in the design.

B. Magnetic Design

The design of the motor requires a permanent magnet bias on the Terfenol. The magnetic design of the Terfenol/magnet stack was driven by two conflicting requirements. The first was a desire to make the bias field as uniform as possible within the stack and the second was a desire to minimize the number of magnets. Increasing the number of magnets has several disadvantages: 1) it increases the parts count, and 2) the increased number of joints in the stack could lead to a loss in the motion of the rod due to compression in the joint region.

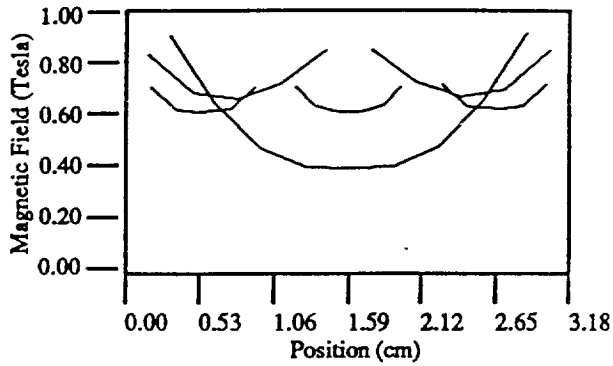

Fig. 4 Results of magnetic analysis for 2, 3 and 4 magnet designs. B is the average induced magnetic bias field in the Terfenol. The x axis gives the position in the stack. The total stack length is 3.18 cms.

The ratio of magnet length to Terfenol length in the stack is fixed by the magnetic bias requirement. Earlier work has shown that best design is to put magnets both in the middle and on the ends. We tried designs with only the end magnets, and one or two magnets inside the rod. Fig. 4 shows the results of calculations using the MSC "Maggie" magnetic analysis program. The difference between the three and four magnet designs was fairly small; it appeared that going to five magnets would not be worth the cost. The final designs used a 0.254 cm magnet at each end and two of 0.381 cm thickness between the internal Terfenol segments. A magnetic tube biasing arrangement was also considered but not fully examined due to space limitations in the motor. The influence of the magnetic fields produced by the circuit on the pusher circuit and vice versa was minimized.

C. Prototype Test Results

The motor was brought to the prototype stage recently. Table 2 shows the test results of the prototype. Even with undersized drive rods prototype yielded a record (for its size of 26 X 11.50 X 10.80 cms) 12.2 N.M of torque directly off its shaft at 0.5 rpm.

Table 2: Prototype Test Results

Dimensions		
Length (cms)	Width (cms)	Height (cms)
26.00	11.50	10.80
Current (Amps)	Voltage (Volts)	Frequency (Hz)
2.15	32.00	225.00
Torque (N.m)	R.P.M.	Step Size (rad.)
0.53	0.16	840 E - 6

The device used 600 watts of power. Rotary motion was achieved and the motor ran smoothly. The holding torque was on the same order of magnitude as the drive torque. And the step resolution was equally outstanding, 800 micro-radians for a full cycle. Low speed (0.5 rpm) compared to the predicted speed (60 rpm) is due to the fact that the prototype is scaled to prove the principle, leading to excessive internal inertia and the fact that only underpowered Terfenol rods, which were available, were used.

Roller Locking Principle

Fig. 5 (a) illustrates the roller locking concept. The drive assembly consists of two concentric races, in which one is circular (drive drum - which is positively connected to output shaft) and other cylinder having cams on its outer rim (drive cam cylinder - which is free to rotate on shaft) with a roller above each cam. Relative rotation which wedges the rollers between the narrow portion of the cam and the circular surface of the outer race forces both races to rotate together, while relative rotation in the opposite direction frees the rollers. For proper locking action, without backlash or slip the condition for self locking $\alpha \leq 2\phi$ must be satisfied. Here α is the angle between tangents to the cam contour and to the roller surface at contact points and $\phi = \tan^{-1} \mu$ (coefficient of friction).

Fig. 5 (b) shows the proposed design in half scale and give an idea of its size and complexity. In order to provide dual directional motion two sets of drive rods and a modified drive cam cylinder is incorporated in the design. The top half of the drive cam cylinder has cam oriented in such a way as to generate counterclockwise (CCW) motion. The bottom half of the drive cam cylinder has cam oriented in reverse fashion to facilitate motion in clockwise (CW) direction.

Under the influence of a magnetic field each of one pair of magnetostrictive rods (A) expands approximately 0.001 cm/cm with great force. The opposing rods (B) contract approximately 0.001 cm/cm. Thus we have a rotational motion of the drive cam cylinder. This drive cam cylinder is coupled to the drive drum by conical rollers. These rollers are lightly preloaded so there is no backlash between the drive cam cylinder and the drive drum. As the drive cam cylinder rotates CCW, the CCW drive rollers try to roll up the CCW drive cams on the drive cam cylinder, but are immediately pinned between the drive drum and the drive cams and the rollers lock generating positive motion in CCW direction. At the same time, the magnets above the CW rollers are activated. Following this, the CW rollers first roll, disengaging from both the drive cam and the drive shaft drum, and then are each pulled up against the magnetized plate. Thus, a preferential CCW torque and motion is established. When the magnetic field in the expanding rod set (A) collapses, the system returns to neutral and the cycle can start again (except that the CW rollers are effectively nonparticipatory). When the magnetic field is excited at high frequency the system cycles in a rapid ratcheting motion generating relatively high rpm. Following the above procedure using the magnetostrictive rod pair (B) as the drive source, results into a CCW ratcheting motion. The torque produced by the magnetostrictive rods is oscillatory while that emerging from the output shaft is unidirectional (but reversible).

A. Expected Performance

1. Torque

Torque capacity for a given geometry of drive drum and drive cam cylinder and their material properties is established by three considerations: Hertz contact stresses, hoop stresses and deflections. The motor design shown in Fig. 5 is arrived at after many iterations to satisfy these requirements. The motor is designed to deliver 81 N.M maximum torque at 156 rpm no load speed. A step size of 2 E - 3 radians is expected from this 12.7 cm dia. and 18 cm long compact package.

2. Frequency Response

No load inertial limitations involve the rollers and drive cam cylinder. We can neglect the drive drum and drive shaft because they store kinetic energy and serve as flywheel. The frequency response of motor under no load depends on the inertia of oscillating parts of motor. Table 3 shows the no load and full load frequency response of motor.

Table 3: No Load and Full Load Frequency Response of Motor

Loading	Acceleration a (rad/sec^2)	Time t(seconds)	Frequency f_m (Hz)	RPM n
No Load	66474.00	2.45E-4	4076.59	155.71
Full Load	30534.70	3.62E-4	2762.92	105.54

3. Structural Stresses and Deformations

As the motor drives, the drive rollers roll slightly, deform and the drum stretches until the structural reactions balance the torque forces. As a rule of thumb this equality of forces should occur before the total deflections exceeds the fifty percent cam rise or Terfenol rod expansion so that useful motion at maximum torque can be achieved. At maximum torque, structural deformations are primarily due to contact and hoop stresses induced in the roller, drive drum and drive cam cylinder. The contact stresses can be reduced by increasing the number of rollers but beyond a certain point it does no good to add additional rollers, since the controlling resisting force that determines torque carrying capacity is the hoop strength and rate of stretch of the drive drum and drive cam cylinder and not the number of rollers involved.

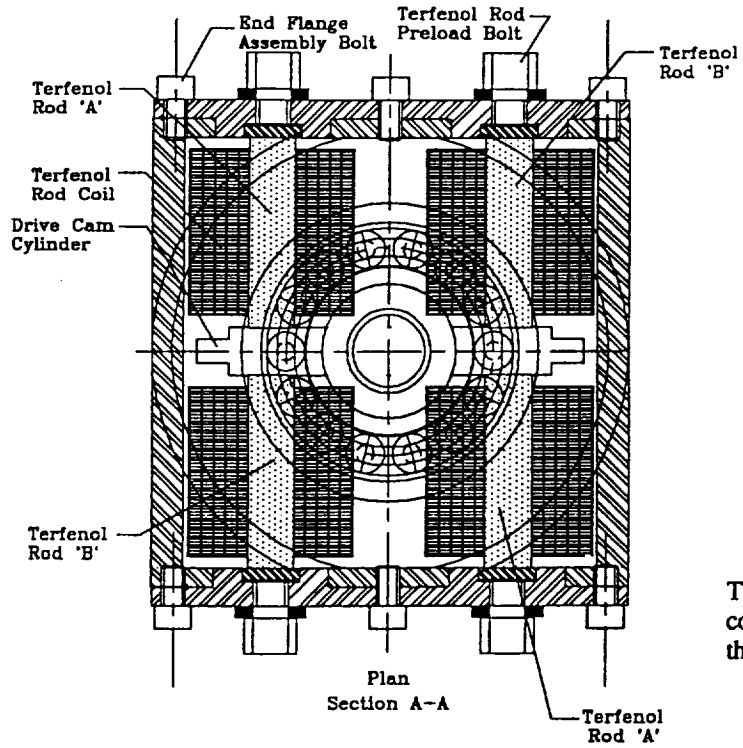

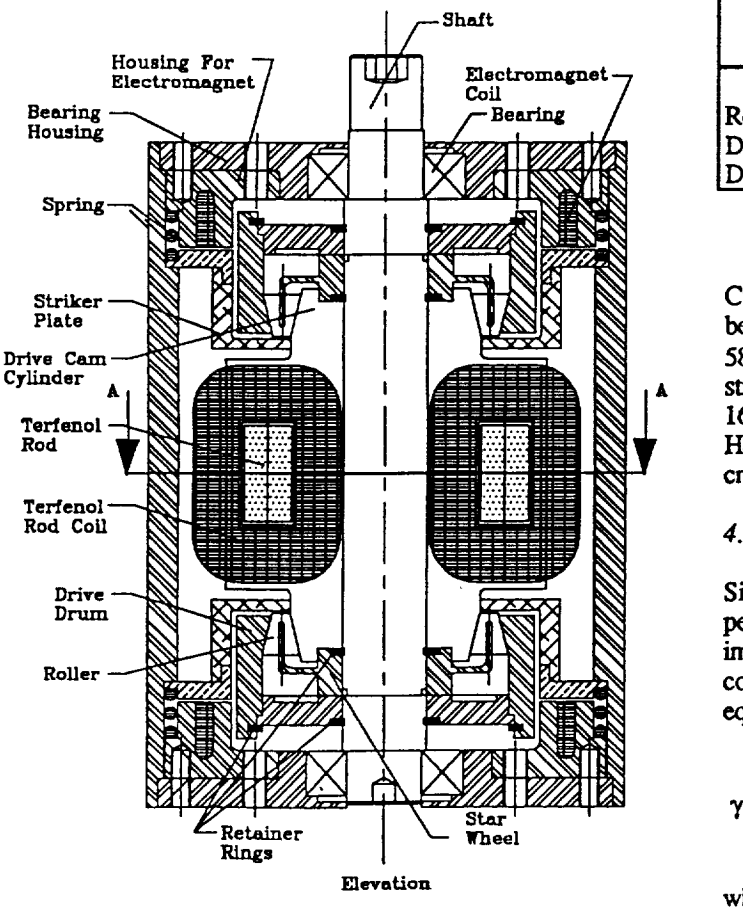

Fig. 5 (b) Magnetostrictive Direct Drive Rotary Motor

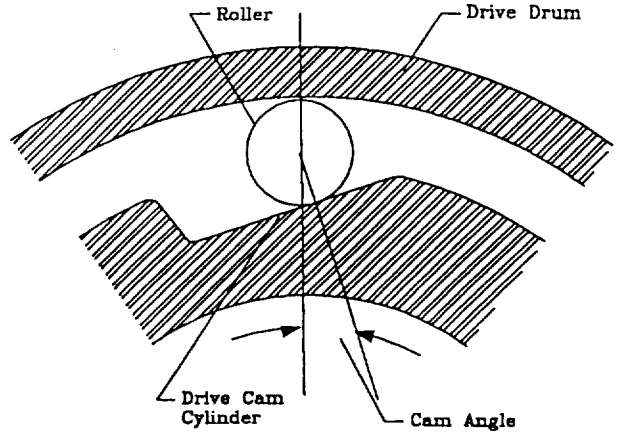

Fig. 5 (a) Roller Locking Concept

The contact stresses and strains and Hoop stresses and strains are computed using appropriate formulae's [9] and are as shown in the following table.

Table 4: Contact and Hoop Stresses for Motor

	Stresses (MPa)		Deformations (μ cms)	
	Contact	Hoop	Contact	Hoop
	σ_c	σ_h	δ_c	δ_h
Roller	-	-	86.36	-
Drive Cylinder	1158.3	12.4	46.74	252.73
Drive Drum	2040.8	53.1	2.11	42.93

$\Sigma \delta = 431.8$ μ cms

Current industry standards limit Hertz stress to 2861 MPa because Brinelling occurs at 4482 MPa for steel hardened to R_c 58-62. Using cam radius larger than roller helps minimize Hertz stresses. The elastic limit for high strength alloy steel is 1207-1655 MPa. Using cam radius larger than roller helps minimize Hertz stresses. The allowable flexure in a half stroke is 455 μ-cms. Thus, deformations appear to be manageable.

4. Wear

Since the wear of various components of roller drive affect the performance and the replacements of these components are impractical, wear and wear predictions are of major concern. The condition for zero wear for N passes is given by following equation [10].

$$\gamma = \left(\frac{2 * 10^3}{N} \right) \gamma_R \qquad (4)$$

where,

$$\gamma = \frac{\tau_{max}}{\tau_y} \quad (5)$$

$$\tau_{max} = \frac{\sigma_{cmax}}{3} \quad (6)$$

γ_R = 0.54 for 2000 passes
σ_{cmax} = Contact stress
τ_{max} = Maximum shear stress
τ_y = Yield strength in shear

Evaluating the above equations for N we get N = 2.4 E07 passes without any significant wear on the cam which is the most vulnerable member of the prototype for wear.

B. Magnetic Design

The motor operates by utilizing two principle, non-intersecting, magnetic circuits. The roller locking system uses an electromagnetically actuated platform to engage each set of rollers, depending on the desired direction of travel. The main magnetostrictive drive circuit consists of a solenoid coil surrounding a stack of 112 oriented Terfenol-D in twinned dendritic sheet form. There is a half closed flux circuit for each of the four assemblies.

The original design and the simplified design that was constructed for prototype were both subjected to an extensive analysis of the relevant magnetic circuits. This analysis included an estimation of magnetic flux concentration, leakage, and interference with other components in the designs. The original design exhibited an inefficient configuration in the central Terfenol-D driving stage. This was eliminated in the simplified prototype. The analysis of the magnetic circuits of the prototype using a 2D model with the MSC Maggie software indicates no particular problems. There is no substantial flux leakage and the magnetic field inside the Terfenol-D driver rod is uniform to within 15%.

C. Prototype Test Results

The original motor is designed for a performance of 81 N.M maximum torque at a no load speed of 156 rpm. A step size of 2 E -3 radians is expected from this 12.7 cm dia. and 18 cm long cylindrical compact package. The critical first step is to prove the principle. A commercial roller-locking device is used to build a unidirectional motor to achieve this objective. The motor was brought to the prototype state recently. The results of the tests on the prototype are as shown in table 5.

Further analysis was carried out to ascertain the actual capability of the prototype. The prototype is capable of producing 107 N.M at 49 RPM in ideal conditions. The maximum displacement was observed at a frequency of 12 Hz. At a frequency of 100 Hz, the prototype showed zero displacement indicating that this frequency matched one of the lowest frequency of the preload springs. Further vibration analysis is being carried out to determine the vibration modes of the prototype.

Table 5: Prototype Test Results

Dimensions		
Length (cms)	Width (cms)	Height (cms)
18.00	21.00	31.50
Current (Amps)	Voltage (Volts)	Frequency (Hz)
4.20	13.50	12.00
Torque (N.M)	R.P.M.	Step Size (rad.)
0.53	0.16	0.0114 E -6

IV. CONCLUSIONS

The prototype demonstrations were highly successful in proving the inch-worm and roller locking principles for magnetostrictive motors. High torque, precision microsteps, self braking and bi-directional rotary motion are the attractive features of these motors.

REFERENCES

[1] Akuta, T.: "An Application of Giant Magnetostrictive Material To High Power Actuators", Tenth International Workshop on Rare Earth Magnets and Their Applications, Kyoto, Japan, (1989).

[2] Kiesewetter, L.: "The Application of Terfenol in Linear Motors", Proceedings of Second International Conference on Giant Magnetostrictive and Amorphous Alloys for Sensors and Applications, (1988).

[3] Tyren, C.: "High Performance Actuators Based on Giant Magnetostrictive Alloys (Terfenol)", VDI/VDE Conference, Actuator 88.

[4] Final Report ARO/DARPA, DAAG 29-85-K-0096.

[5] Panasonic Technical Reference on the Ultrasonic Motor, Panasonic Industrial Company, Electric Motor Division. Matsushita Electric Industrial Co., Ltd. Osaka 574 Japan.

[6] Ida, N. and Roemer, L.E.: "A Magnetostrictive Motor", Journal of Applied Physics, No. 63 Vol. 8, pp. 3989-3990, (1988).

[7] Huang, K., Report on " Design Guidelines for Terfenol Actuators", Institut fur Feinwerktechnik an der Technischen, Universitat Berlin, (1988).

[8] Butler, J. L., "Application Manual For The Design of Terfenol-D Magnetostrictive Transducers", Prepared for Edge Technologies Inc., (1987).

[9] Young, W.C.: "Roark's Formulas for Stress and Strain", McGraw Hill, sixth edition, (1989).

[10] McGregor, C.W. (Ed.): "Handbook of Analytical Design For Wear", Plenum Press, N.Y., pp. 2, (1964).

Section II
Programmable Slip Clutch/Brake

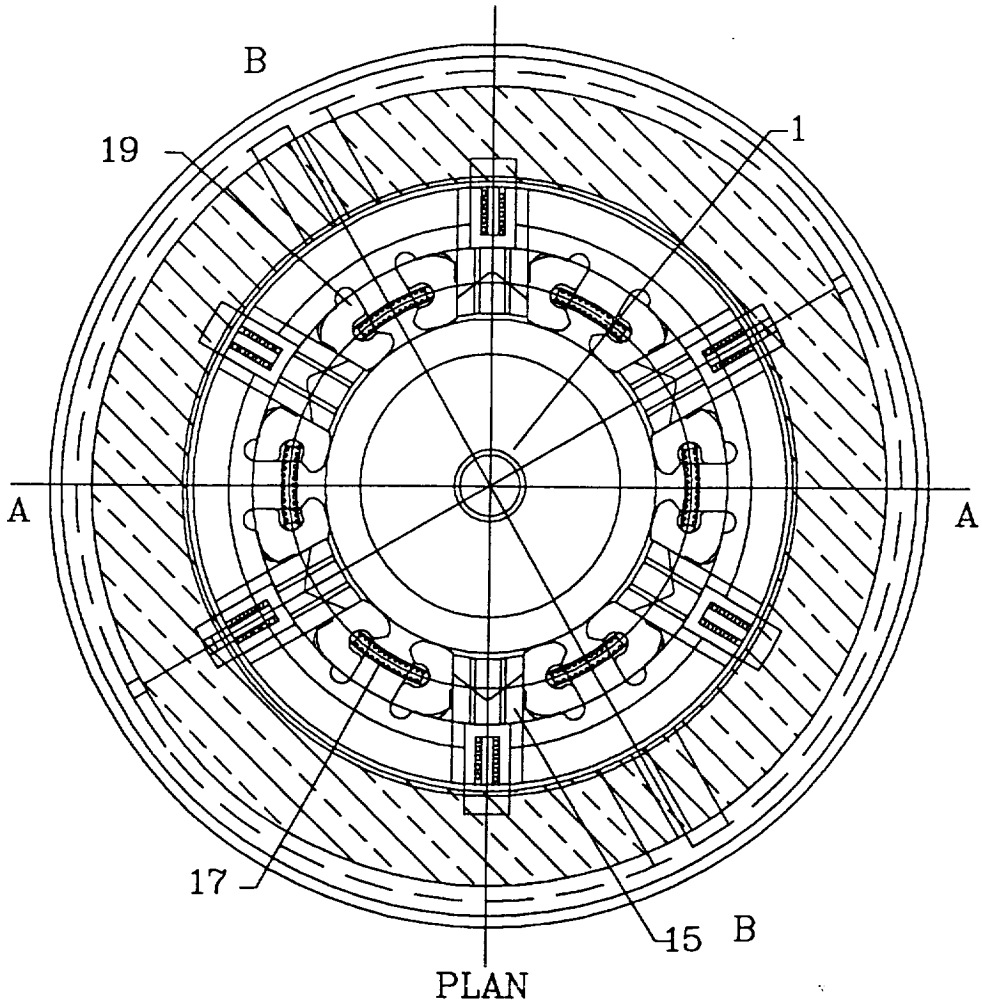

PLAN

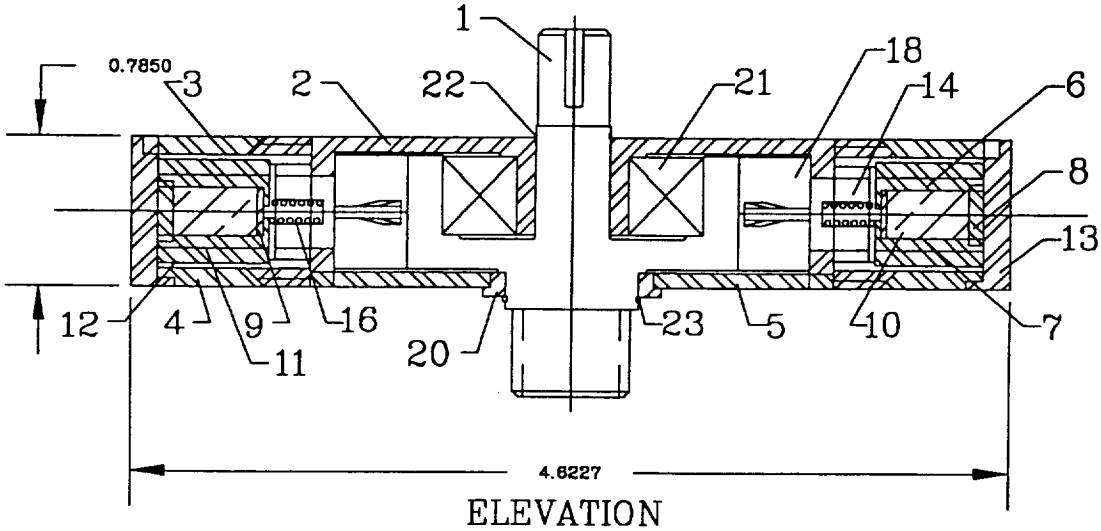

ELEVATION

ITEM NO	REQ'D	REQ'D	PART NO	DESCRIPTION	MATERIAL	MATERIAL SPEC.
23	1		NAG 5-1169-23	RETAINING RING	3AMI-9	
22	1		NAG 5-1169-22	RETAINING RING	3AMI-5	
21	1		NAG 5-1169-21	BEARING	FAG 6202.2RSR	
20	1		NAG 5-1169-20	BUSHING	SAE 791	
19	12		NAG 5-1169-19	SPRAG LOCATING GEAR	SAE 4027	
18	12		NAG 5-1169-18	SPRAG	T2	
17	6		NAG 5-1169-17	SPRAG PRELOAD SPRING	SAE 1060	
16	6		NAG 5-1169-16	STRIKER LOCATING SPRING	SAE 1060	
15	12		NAG 5-1169-15	STRIKER	T2	
14	6		NAG 5-1169-14	STRIKER	T2	
13	1		NAG 5-1169-13	CASING	SAE 4640	
12	2		NAG 5-1169-12	SOLENOID SUPPORT PLATE (BOTTOM)	AISI 1074	
11	2		NAG 5-1169-11	SOLENOID SUPPORT PLATE (TOP)	AISI 1074	
10	1		NAG 5-1169-10	SOLENOID COIL	AWG 22	
9	2		NAG 5-1169-09	SOLENOID COIL SUPPORT CYLINDER	SAE 30302	
8	2		NAG 5-1169-08	SOLENOID CYLINDER	ALLOY 48	
7	2		NAG 5-1169-07	SOLENOID PLATE (BOTTOM)	ALLOY 48	
6	2		NAG 5-1169-06	SOLENOID PLATE (TOP)	ALLOY 48	
5	1		NAG 5-1169-05	BOTTOM COVER	AISI 1085	
4	1		NAG 5-1169-04	BOTTOM FLANGE	AISI 4620	
3	1		NAG 5-1169-03	TOP FLANGE	AISI 4620	
2	1		NAG 5-1169-02	OUTER RACE	T2	
1	1		NAG 5-1169-01	SHAFT	T2	

LIST OF MATERIAL

NASA (GSFC)/UNCC: NAG 5-1169

UNLESS OTHERWISE SPECIFIED DIMENSIONS ARE IN INCHES

TOLERANCES:

.XX	.XXX	∠	FRACTIONS	
±0.01	±0.005	±1°	±1/16	125√

REMOVE ALL BURRS AND SHARP EDGES 0.01R OR CHAMFER MAX

- ☐ NO NON-DESTRUCTIVE EXAMINATION (NDE) REQ'D
- ☐ STANDARD NDE REQUIRED PER _____
- ☐ SPECIAL NDE REQUIRED PER _____

NAME	INIT	DATE
DESIGNER		
DRAWN		
CHECKED		
APPROVED		
APPROVED		
APPROVED		
APPROVED ENGINEER		

DRAWING INTERPRETED PER GSFC--X873-84-1

PROGRAMMABLE
SLIP CLUTCH
(Radial Set-Up)

NEXT ASSY	USED ON
	ROBOTICS

CODE 718	SCALE 1:1	WT	SH OF

ITEM NO	REQ'D	REQ'D	PART NO	DESCRIPTION	MATERIAL	MATERIAL SPEC.
16	6		NAG 5-1169-16	STRIKER LOCATING SPRING	SAE 1060	
15	12		NAG 5-1169-15	STRIKER	T2	
14	6		NAG 5-1169-14	STRIKER	T2	
13	1		NAG 5-1169-13	CASING	SAE 4640	
12	2		NAG 5-1169-12	SOLENOID SUPPORT PLATE (BOTTOM)	AISI 1074	
11	2		NAG 5-1169-11	SOLENOID SUPPORT PLATE (TOP)	AISI 1074	
10	1		NAG 5-1169-10	SOLENOID COIL	AWG 22	
9	2		NAG 5-1169-09	SOLENOID COIL SUPPORT CYLINDER	SAE 30302	
8	2		NAG 5-1169-08	SOLENOID CYLINDER	ALLOY 48	
7	2		NAG 5-1169-07	SOLENOID PLATE (BOTTOM)	ALLOY 48	
6	2		NAG 5-1169-06	SOLENOID PLATE (TOP)	ALLOY 48	
5	1		NAG 5-1169-05	BOTTOM COVER	AISI 1085	
4	1		NAG 5-1169-04	BOTTOM FLANGE	AISI 4620	
3	1		NAG 5-1169-03	TOP FLANGE	AISI 4620	
2	1		NAG 5-1169-02	OUTER RACE	T2	
1	1		NAG 5-1169-01	SHAFT	T2	

LIST OF MATERIAL

NASA (GSFC)/UNCC: NAG 5-1169

UNLESS OTHERWISE SPECIFIED DIMENSIONS ARE IN INCHES

TOLERANCES:

.XX	.XXX	∠	FRACTIONS	
±0.01	±0.005	±1°	±1/16	125√

REMOVE ALL BURRS AND SHARP EDGES 0.01R OR CHAMFER MAX.

- ☐ NO NON-DESTRUCTIVE EXAMINATION (NDE) REQ'D
- ☐ STANDARD NDE REQUIRED PER _____
- ☐ SPECIAL NDE REQUIRED PER _____

NAME	INIT	DATE
DESIGNER		
DRAWN		
CHECKED		
APPROVED		
APPROVED		
APPROVED		
APPROVED ENGINEER		

DRAWING INTERPRETED PER GSFC-X673-64-1

PROGRAMMABLE
SLIP CLUTCH
(Radial Set-Up)

NEXT ASSY	USED ON	CODE 716	SCALE 1:1	WT	SH OF
	ROBOTICS				

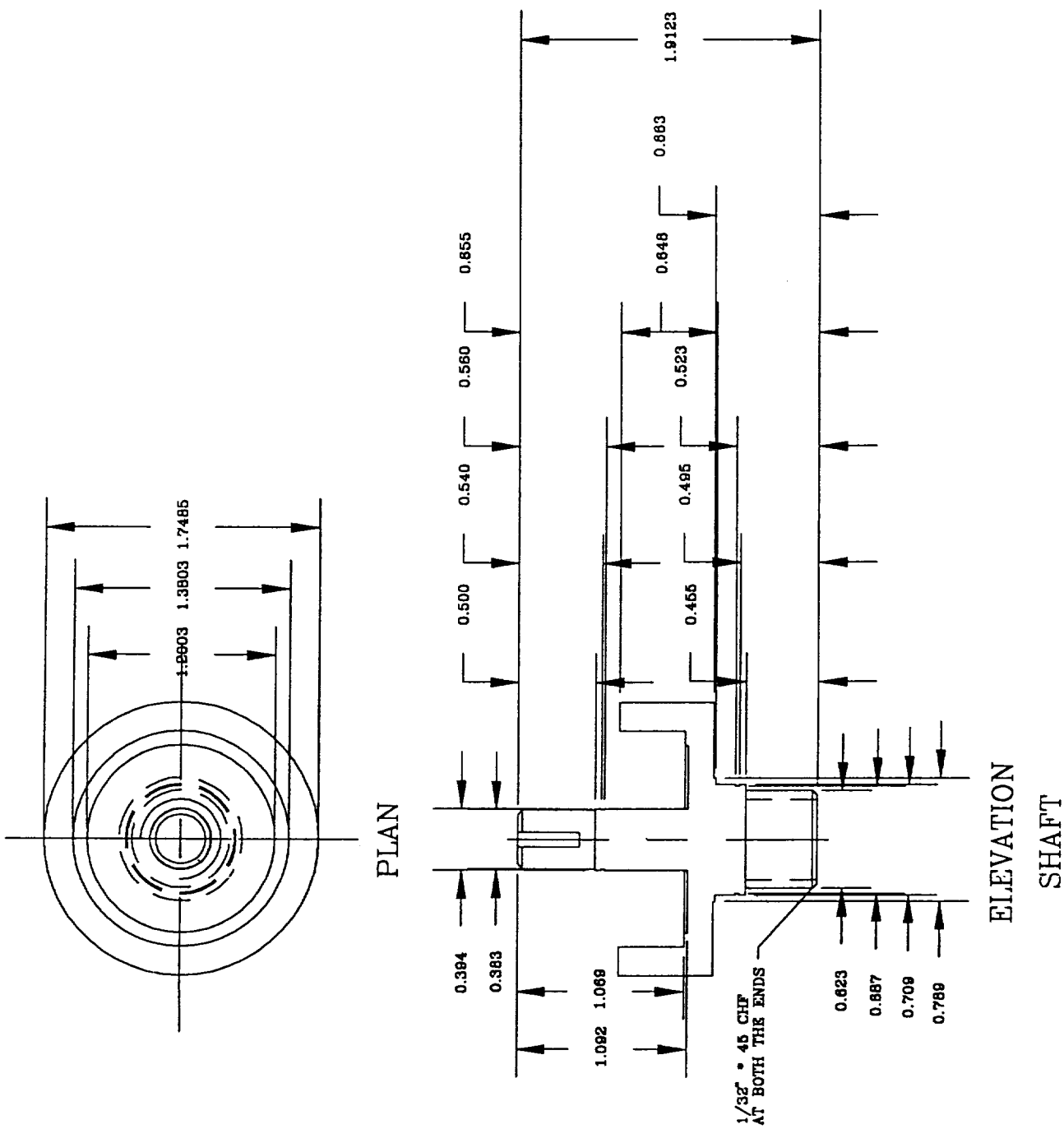
1.7485
1.3803
1.2803
PLAN
1.9123
0.883
0.855
0.848
0.560
0.523
0.540
0.495
0.500
0.455
0.384
0.383
1.092
1.069
1/32" * 45 CHF
AT BOTH THS ENDS
0.623
0.887
0.709
0.789
ELEVATION
SHAFT

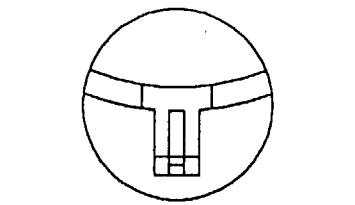

PLAN

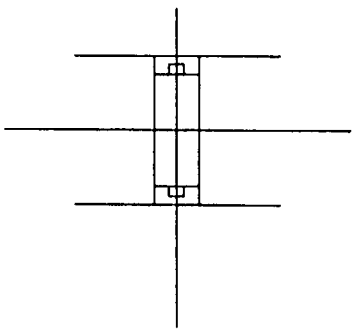

DETAILS B–B

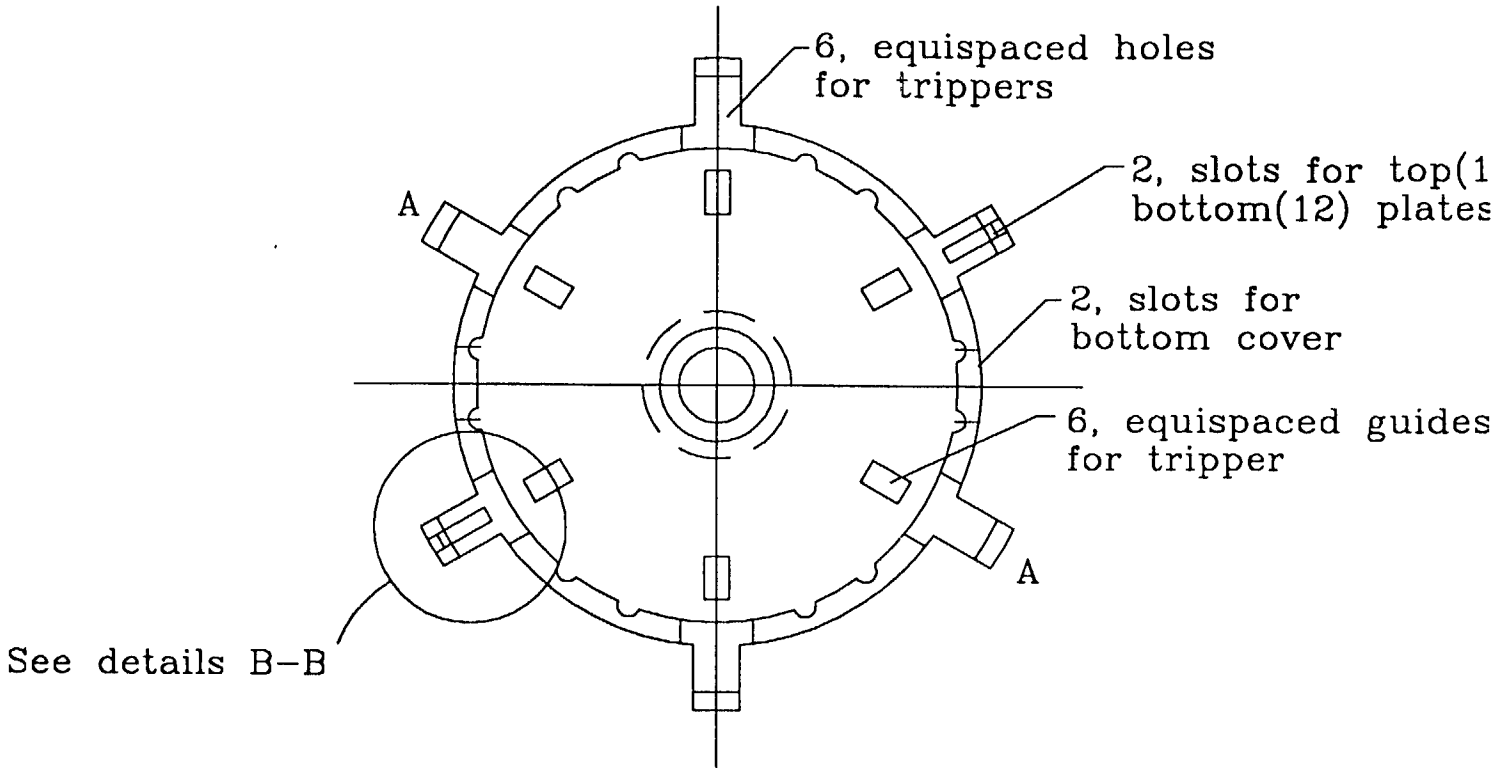

PLAN

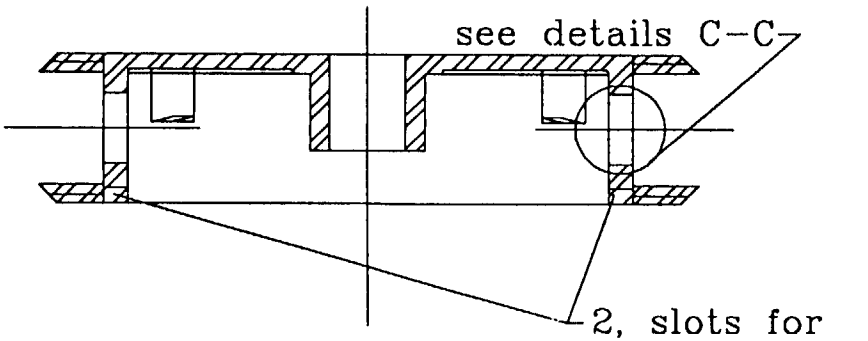

ELEVATION

OUTER RACE

DETAILS C–C

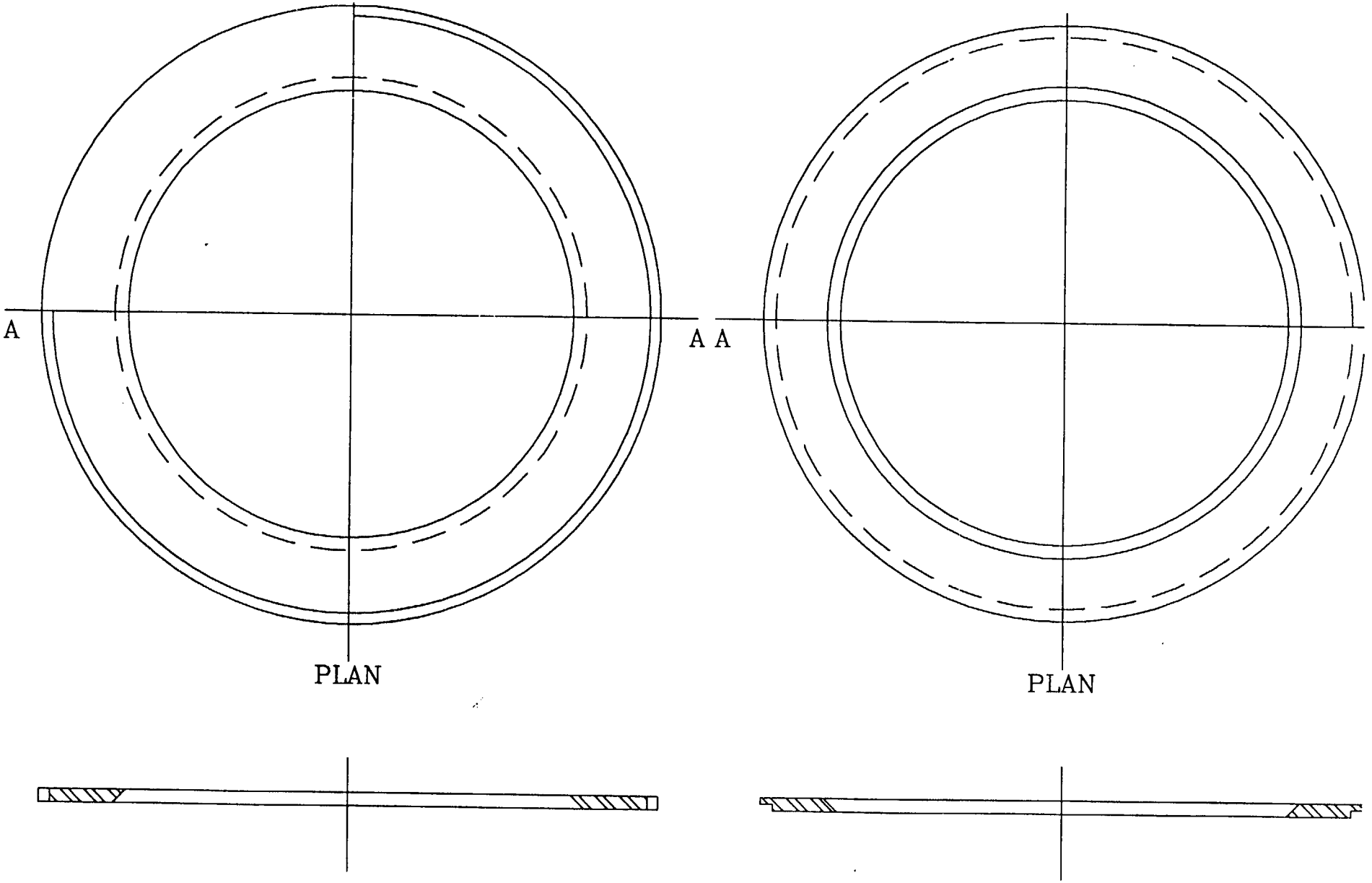

ELEVATION
TOP FLANGE

ELEVATION
BOTTOM FLANGE

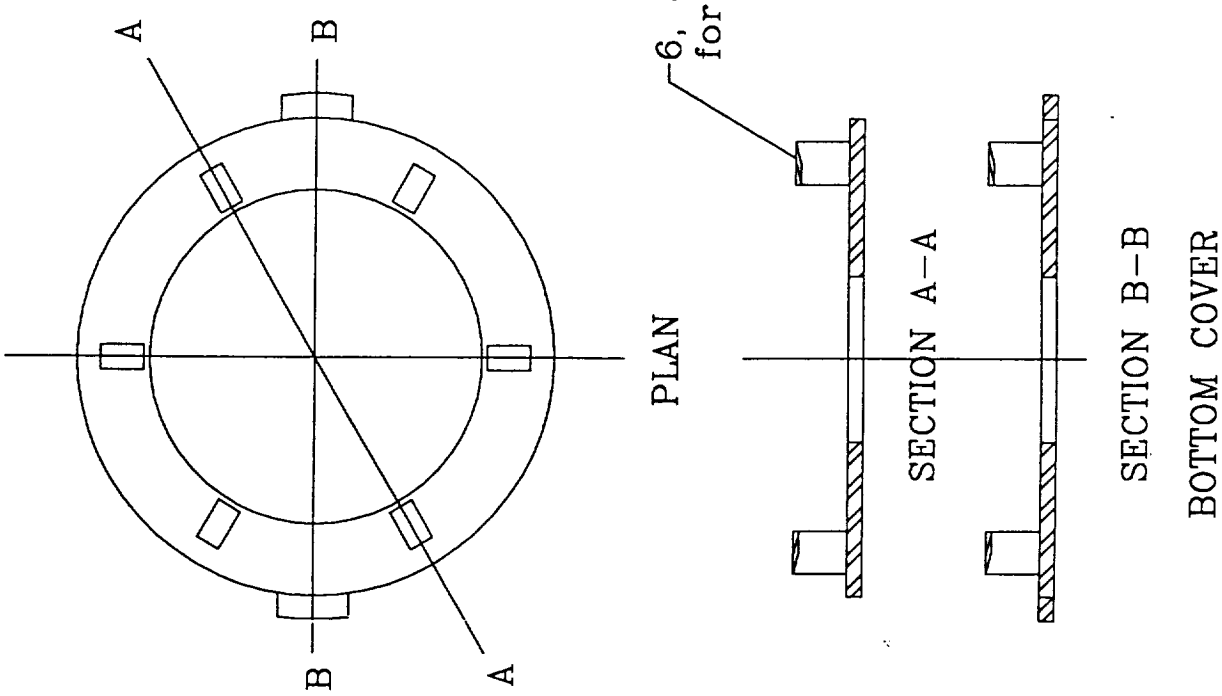
A
B
B
A
PLAN
6, equispaced guides for tripper
SECTION A–A
SECTION B–B
BOTTOM COVER

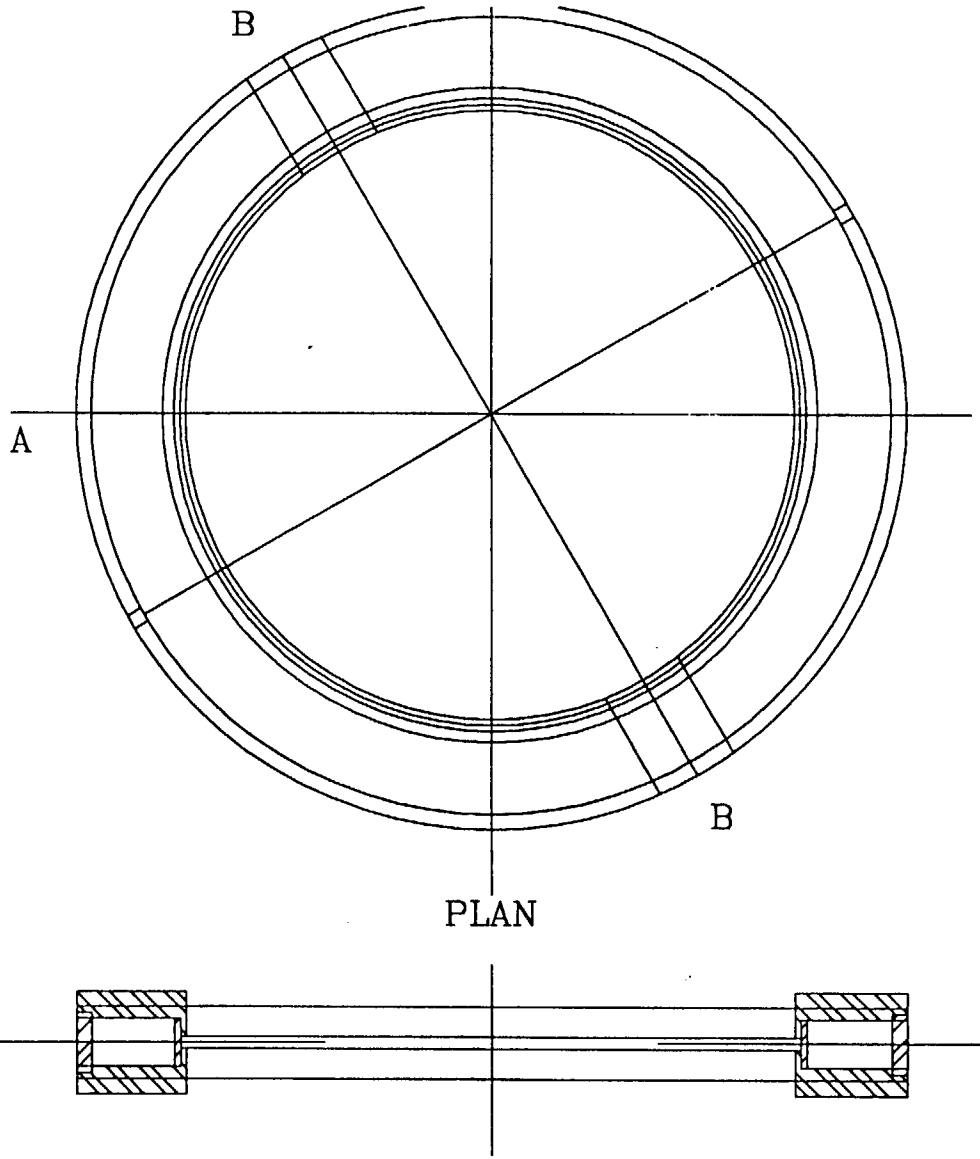

PLAN

ELEVATION

SECTION B–B

SOLENOID

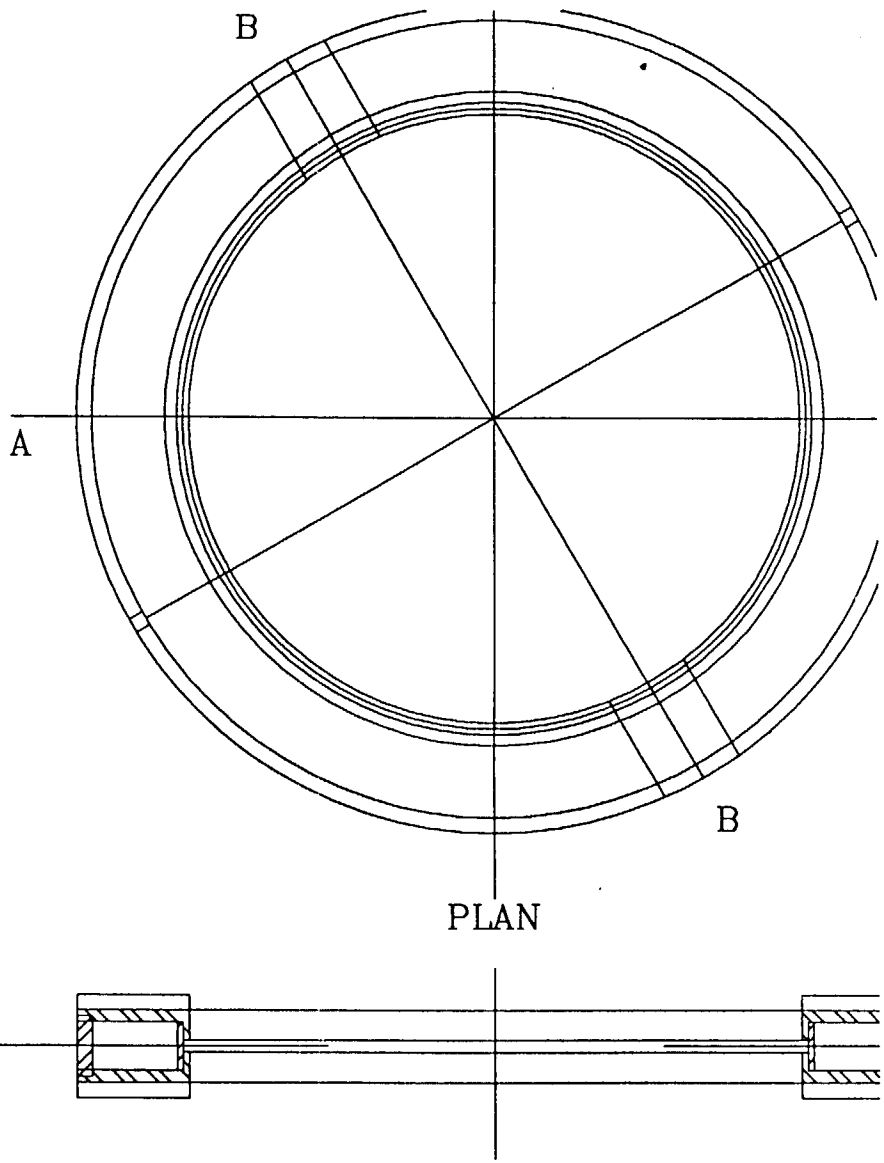

PLAN

ELEVATION

SECTION A–A

SOLENOID

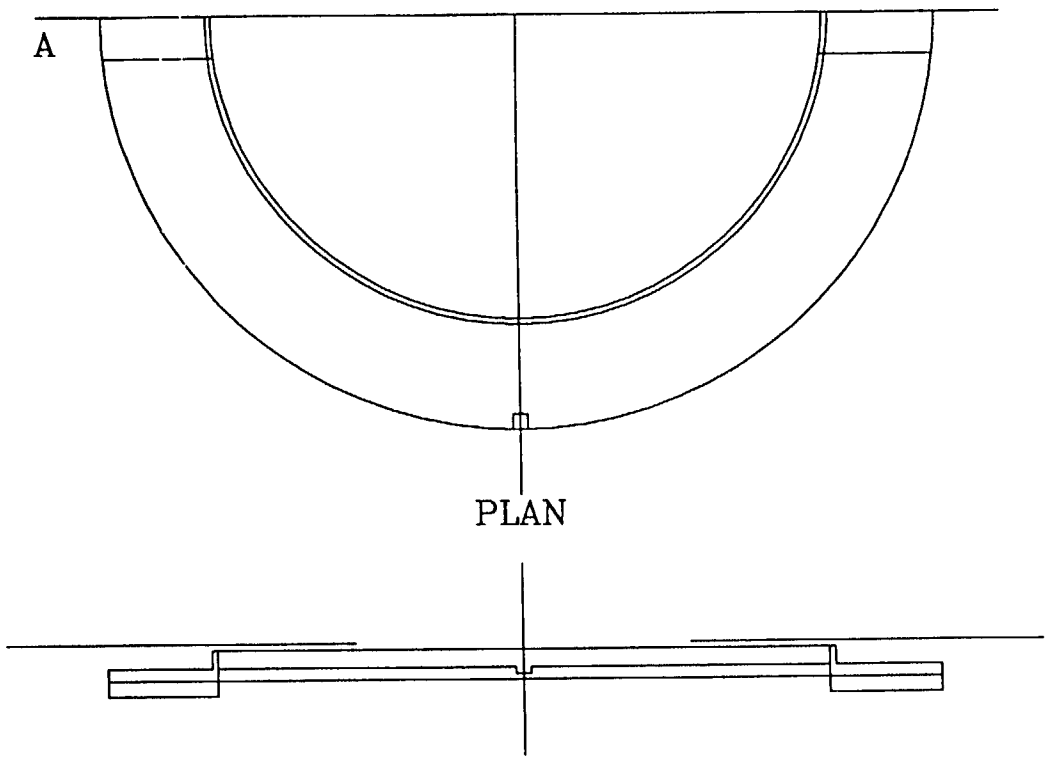

ELEVATION

SECTION A–A

SOLENOID PLATE (BOTTOM)

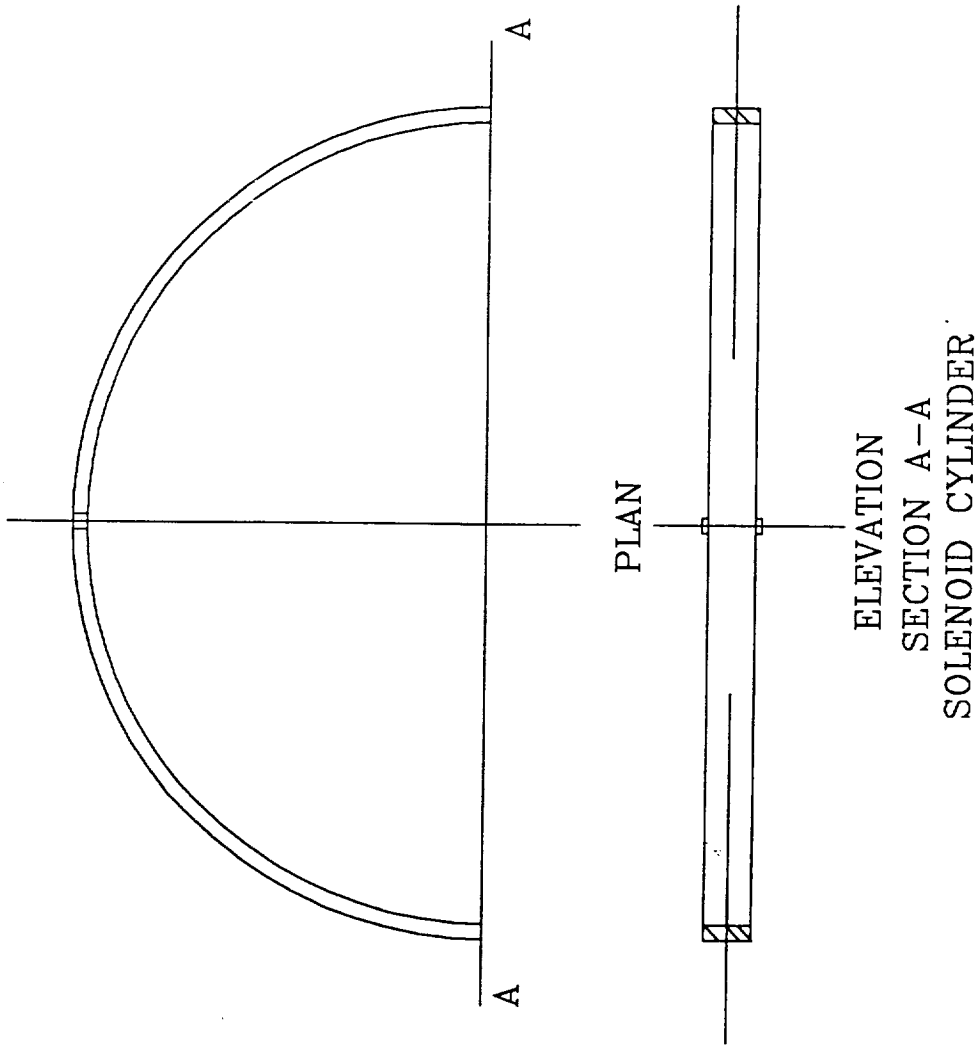
A
A
PLAN
ELEVATION
SECTION A-A
SOLENOID CYLINDER

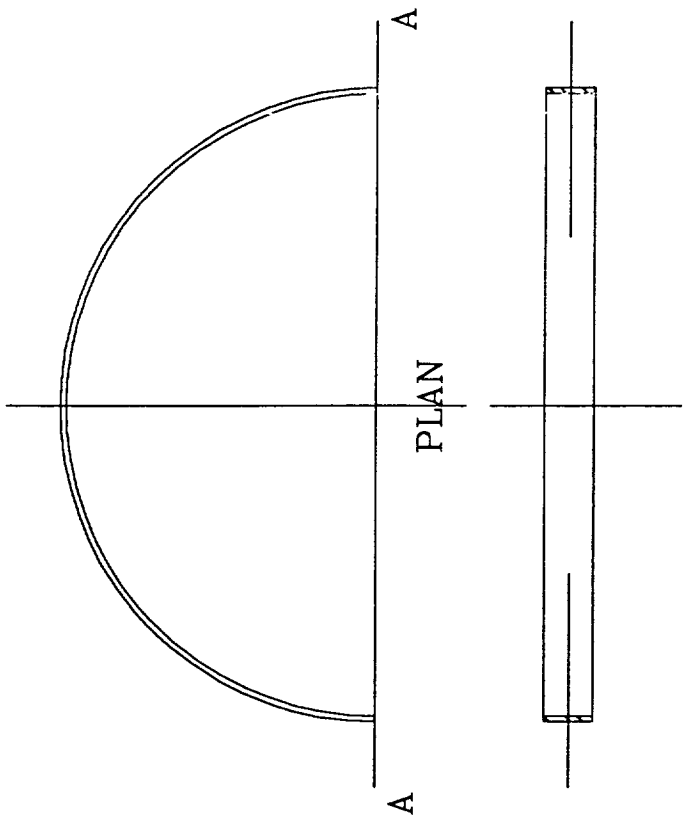

SOLENOID COIL SUPPORT CYLINDER

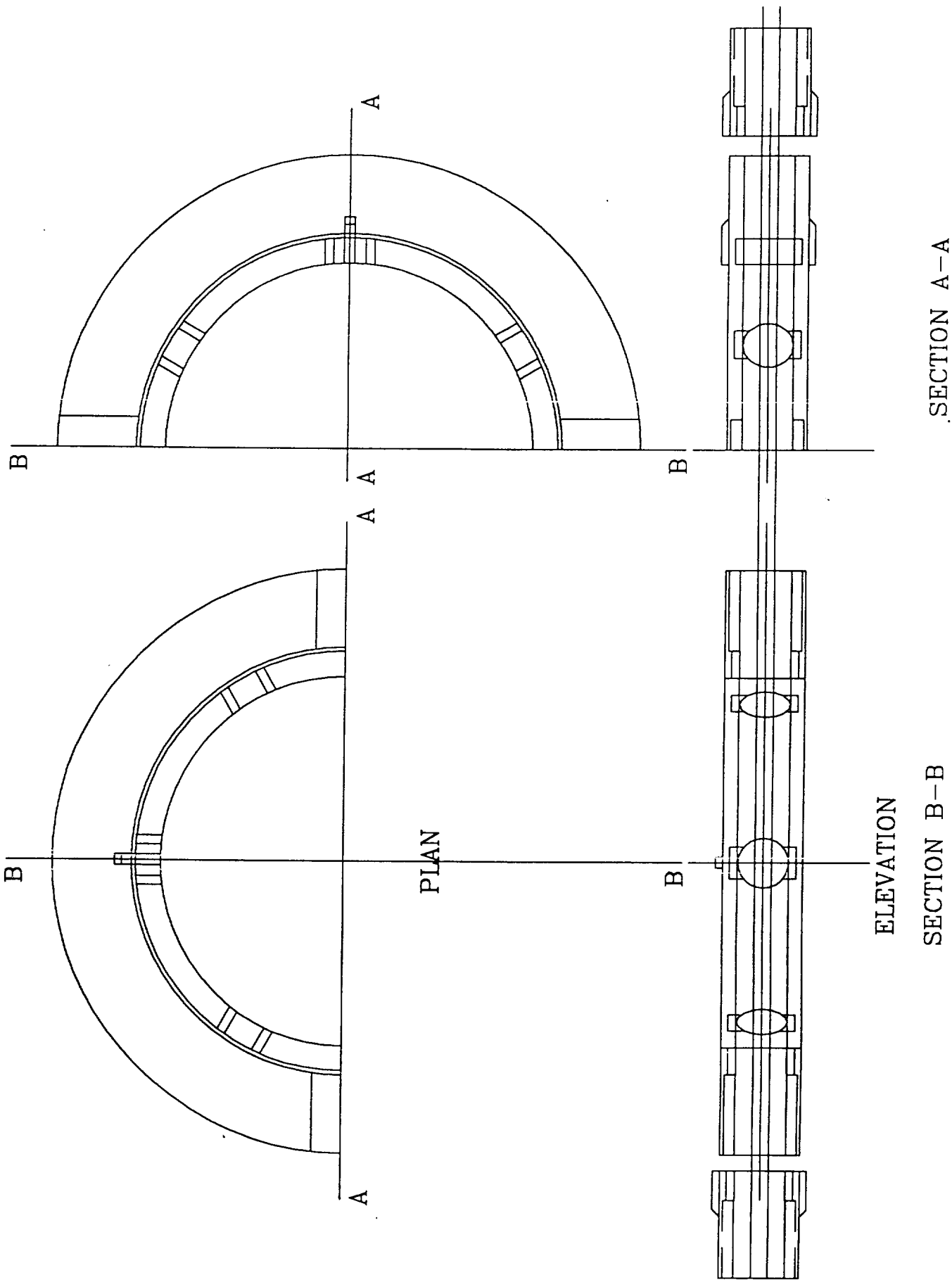
A
B
A
B
PLAN
A
B
ELEVATION
SECTION A–A
SECTION B–B

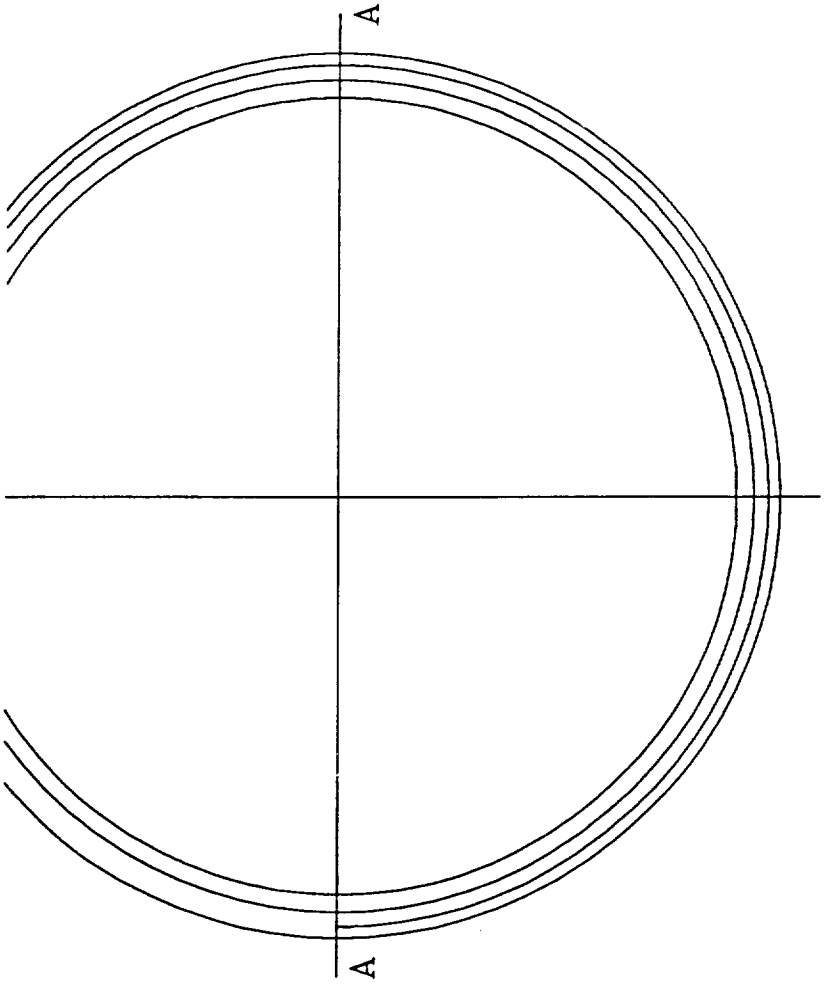

PLAN

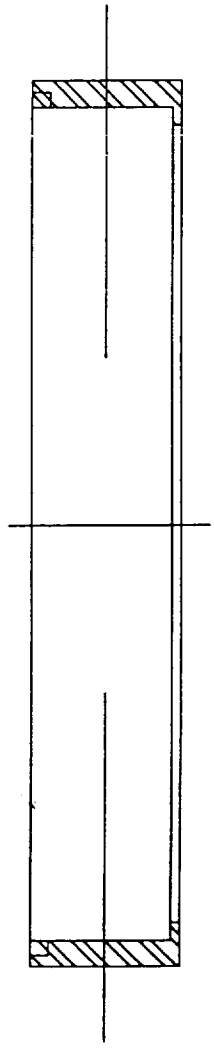

ELEVATION
CASING

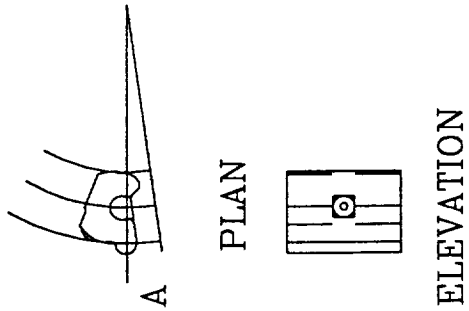
A
PLAN
ELEVATION

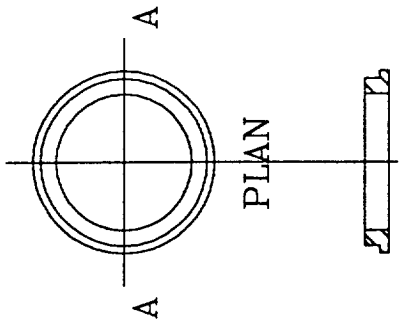
A
A
PLAN
ELEVATION
BUSHING

Section III
Linear Actuator

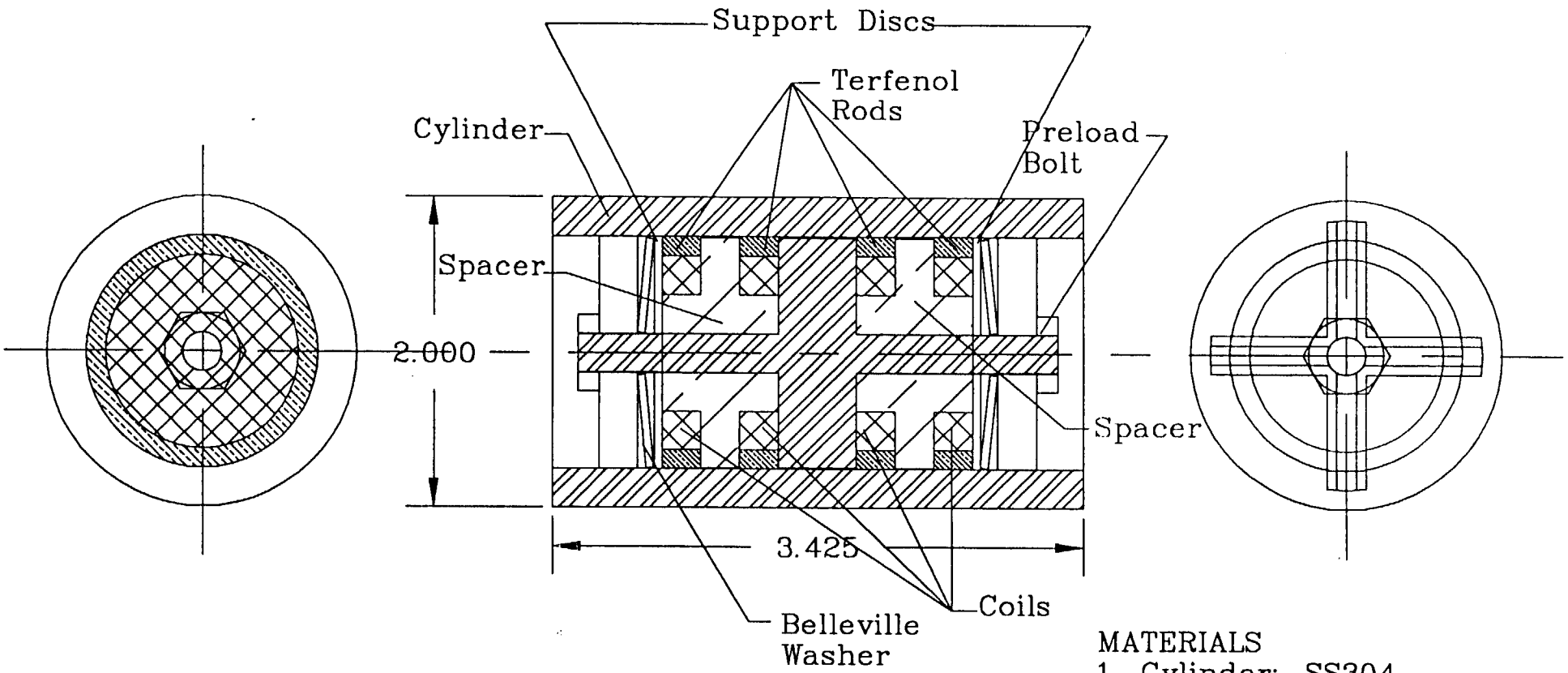

Linear Actuator

Note: Terfenol rods are hollow cylinders.

MATERIALS
1. Cylinder: SS304
2. Spacer: Carbon Steel
3. Spacer: Carbon Steel
4. Belleville Washer: Carbon
5. Preload Bolt: Carbon Ste
6. Coil: 22 Ga.
7. Support Disc: Carbon Ste

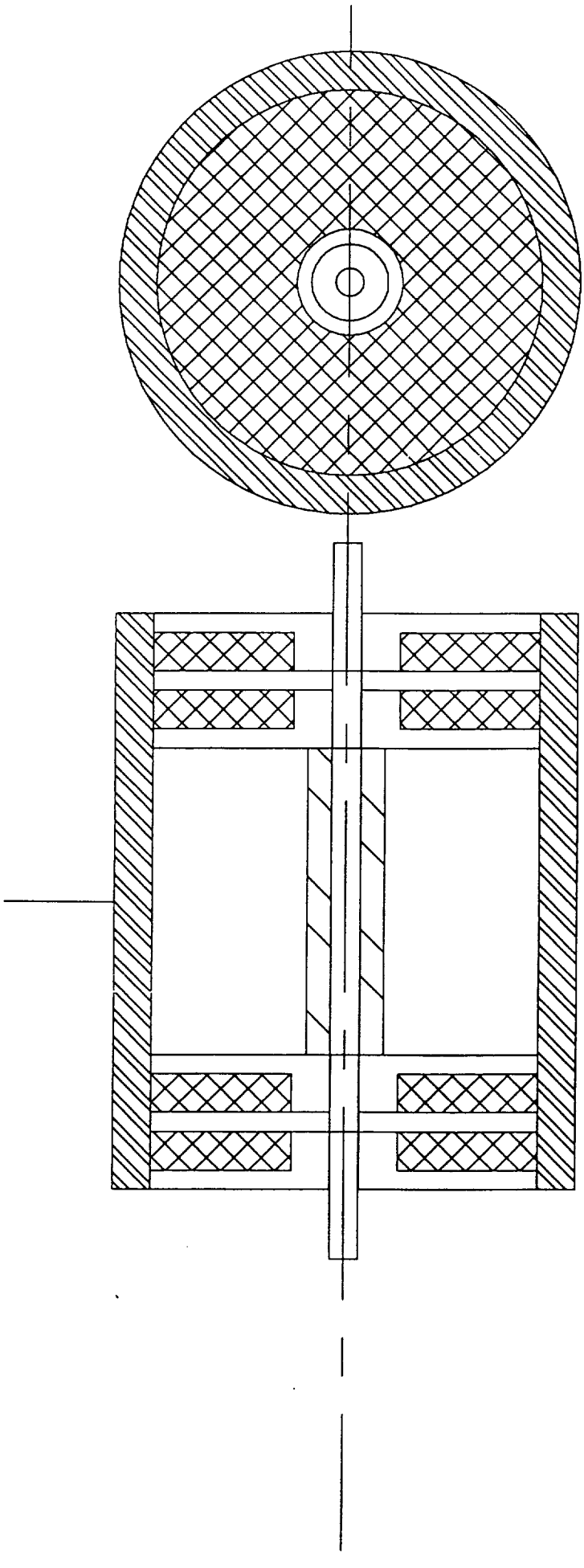

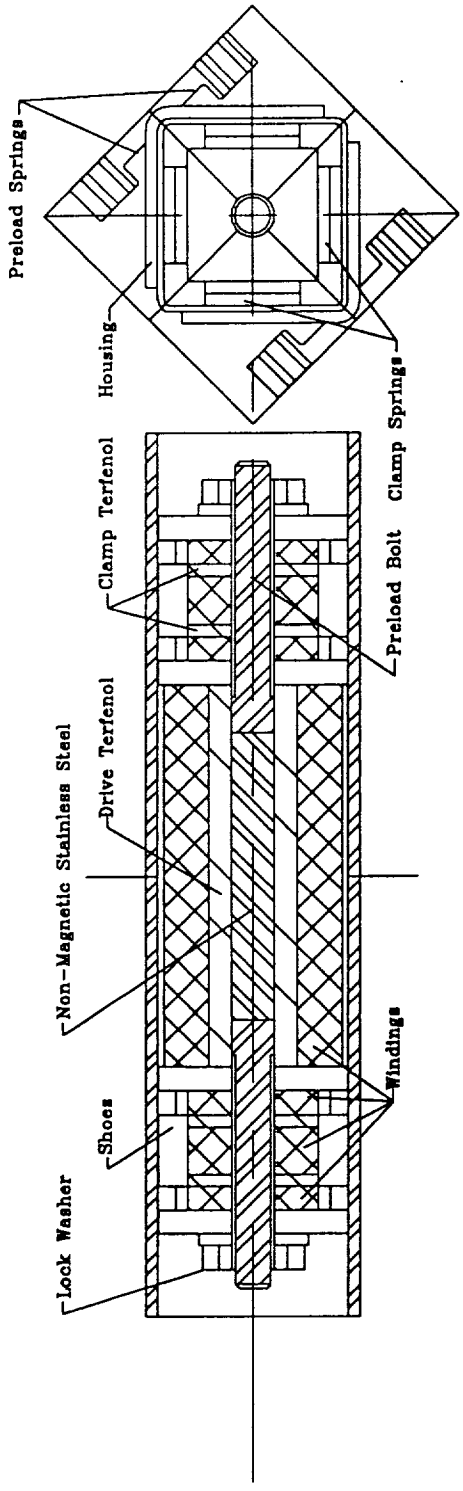
Preload Springs
Housing
Clamp Springs
SIDE VIEW
Clamp Terfenol
Preload Bolt
Drive Terfenol
Non-Magnetic Stainless Steel
Windings
Shoes
Lock Washer
ELEVATION

LINEAR ACTUATOR

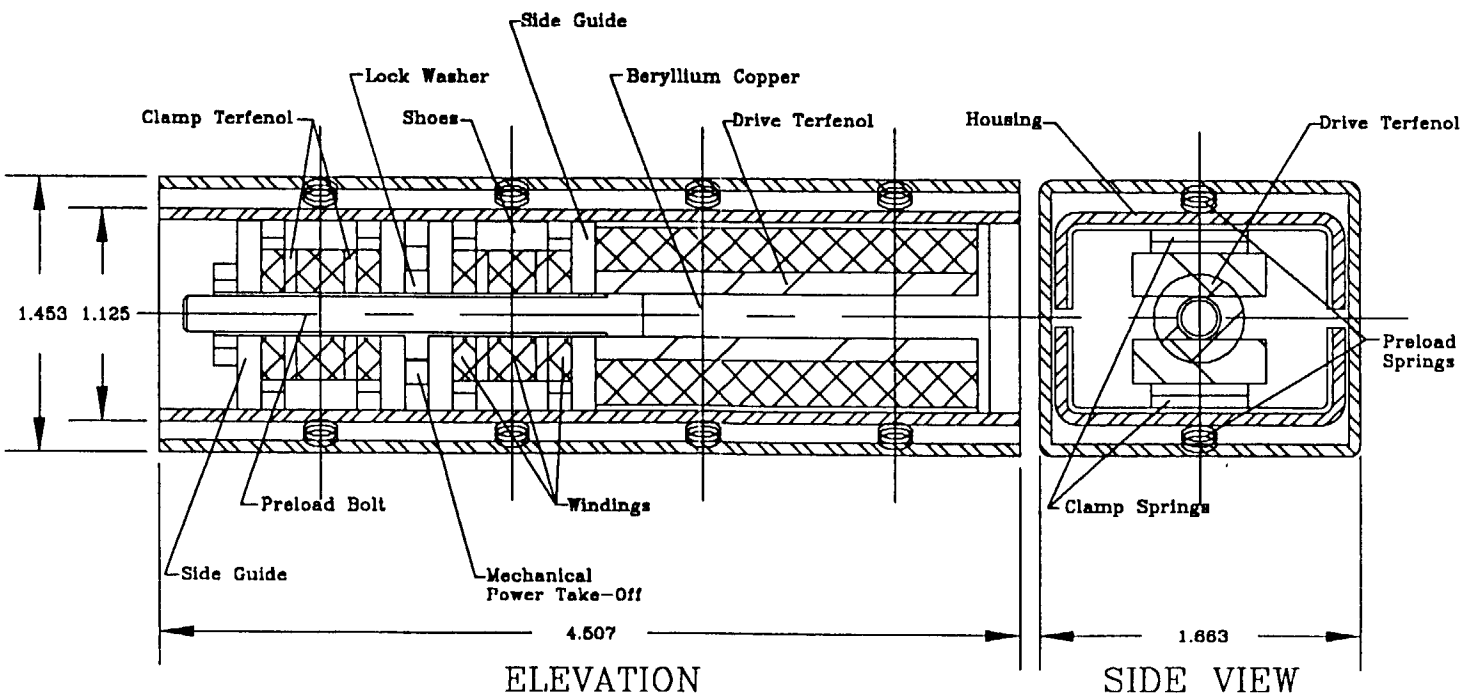

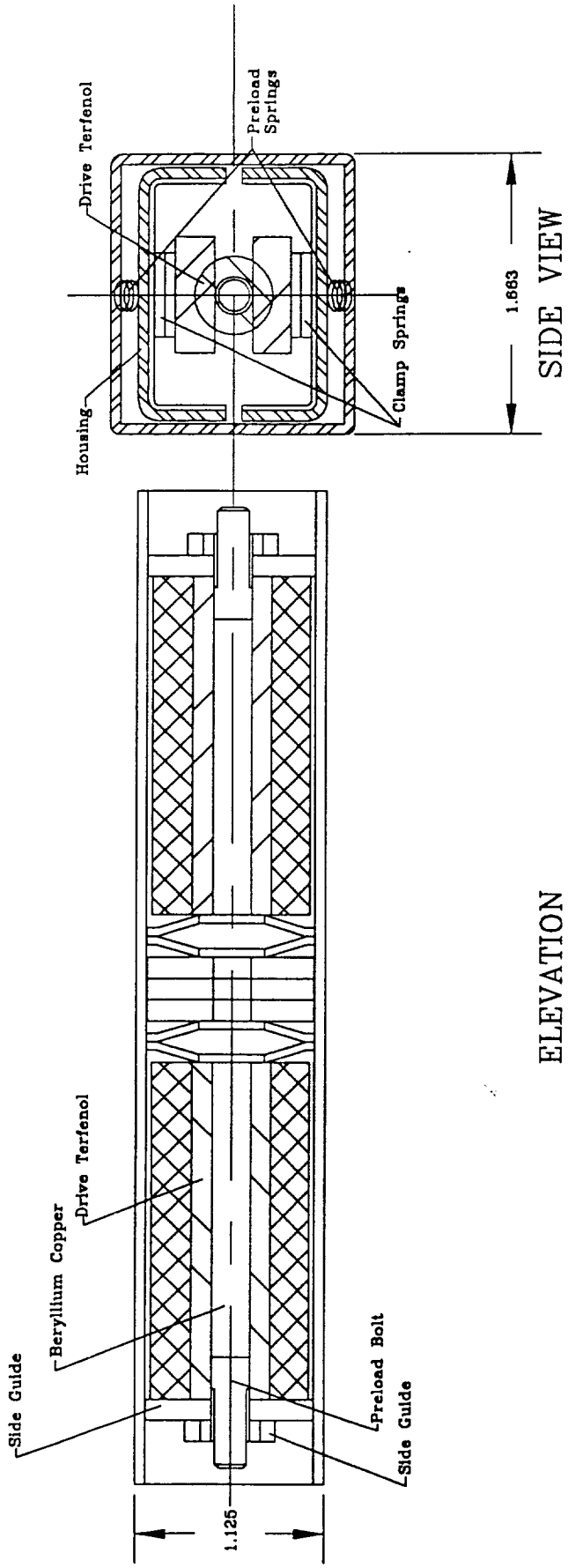
LINEAR ACTUATOR
Drive Terfenol
Preload Springs
Housing
Clamp Springs
1.663
SIDE VIEW
Drive Terfenol
Beryllium Copper
Side Guide
Preload Bolt
Side Guide
1.125
ELEVATION

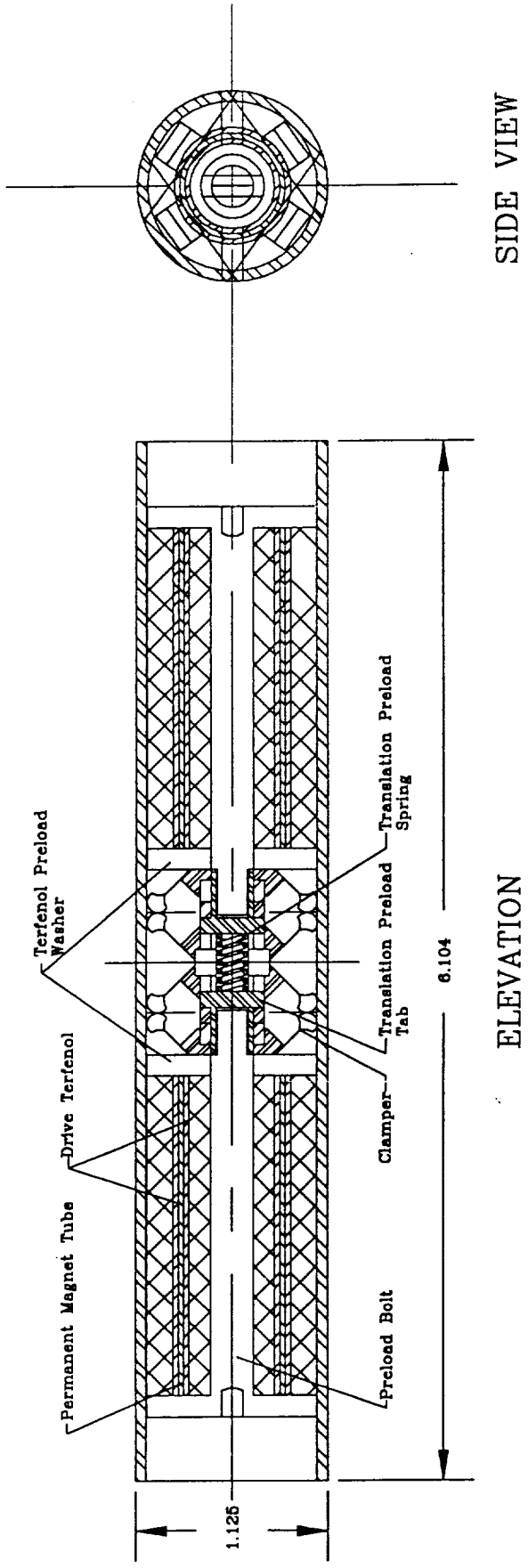
LINEAR ACTUATOR
SIDE VIEW
ELEVATION
Terfenol Preload Washer
Drive Terfenol
Permanent Magnet Tube
Translation Preload Spring
Translation Preload Tab
Clamper
Preload Bolt
6.104
1.125

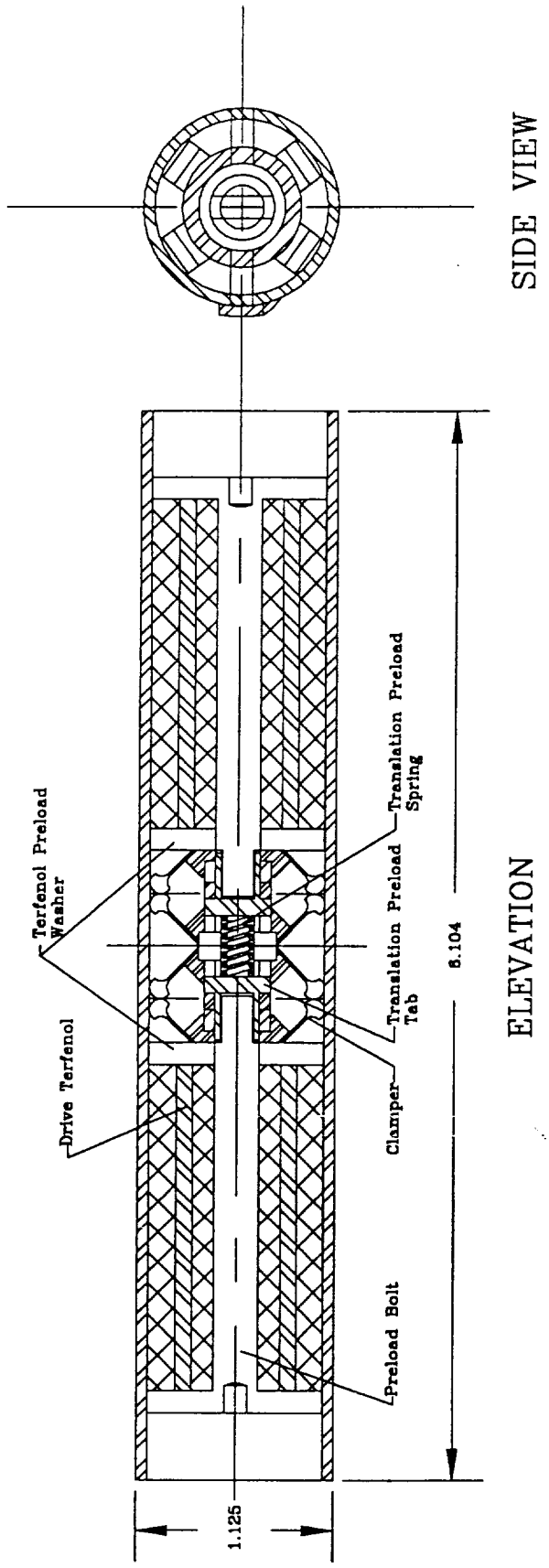
LINEAR ACTUATOR
SIDE VIEW
ELEVATION
Terfenol Preload Washer
Drive Terfenol
Translation Preload Spring
Translation Preload Tab
Clamper
Preload Bolt
8.104
1.125

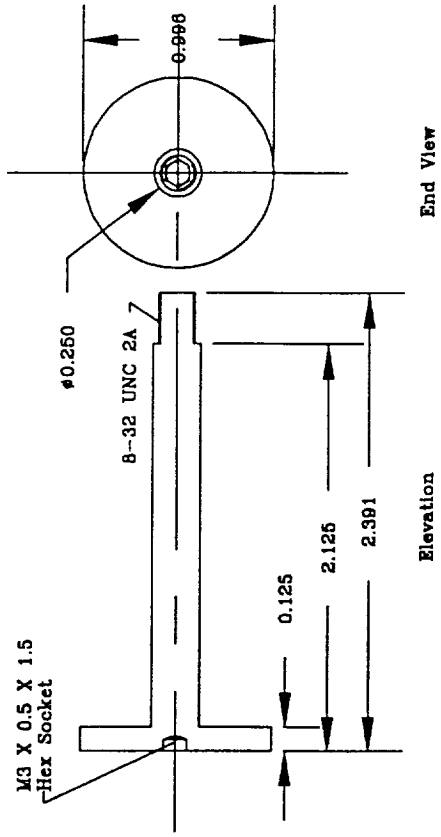
0.998
End View
ø0.250
8-32 UNC 2A
0.125
2.125
2.391
Elevation
M3 X 0.5 X 1.5
Hex Socket

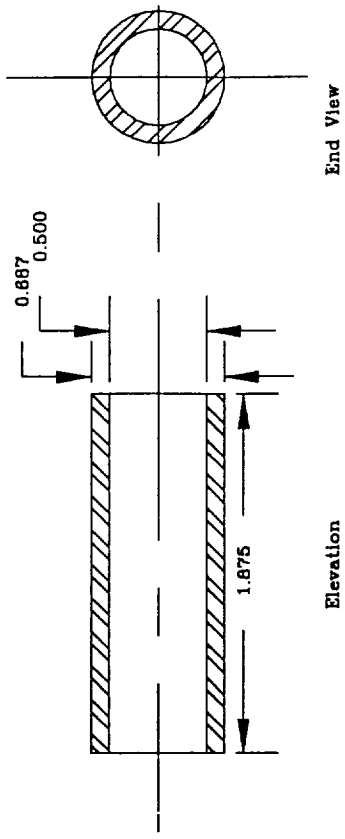
End View
0.887
0.500
1.875
Elevation

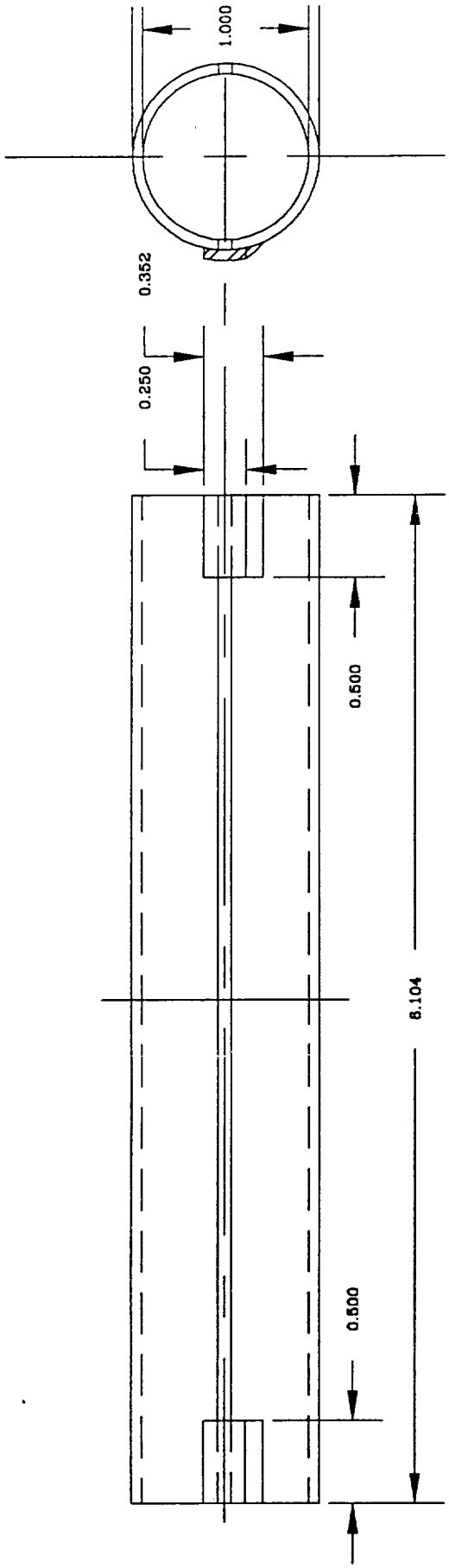

SIDE VIEW

ELEVATION

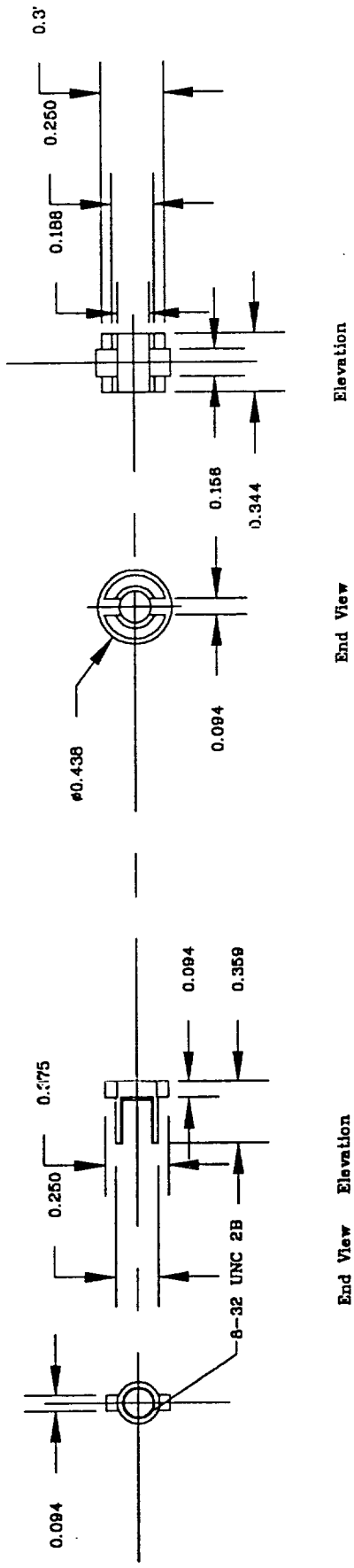
0.3
0.250
0.188
0.158
0.344
Elevation
End View
ø0.438
0.094
0.094
0.359
0.175
0.250
8-32 UNC 2B
End View
Elevation
0.094

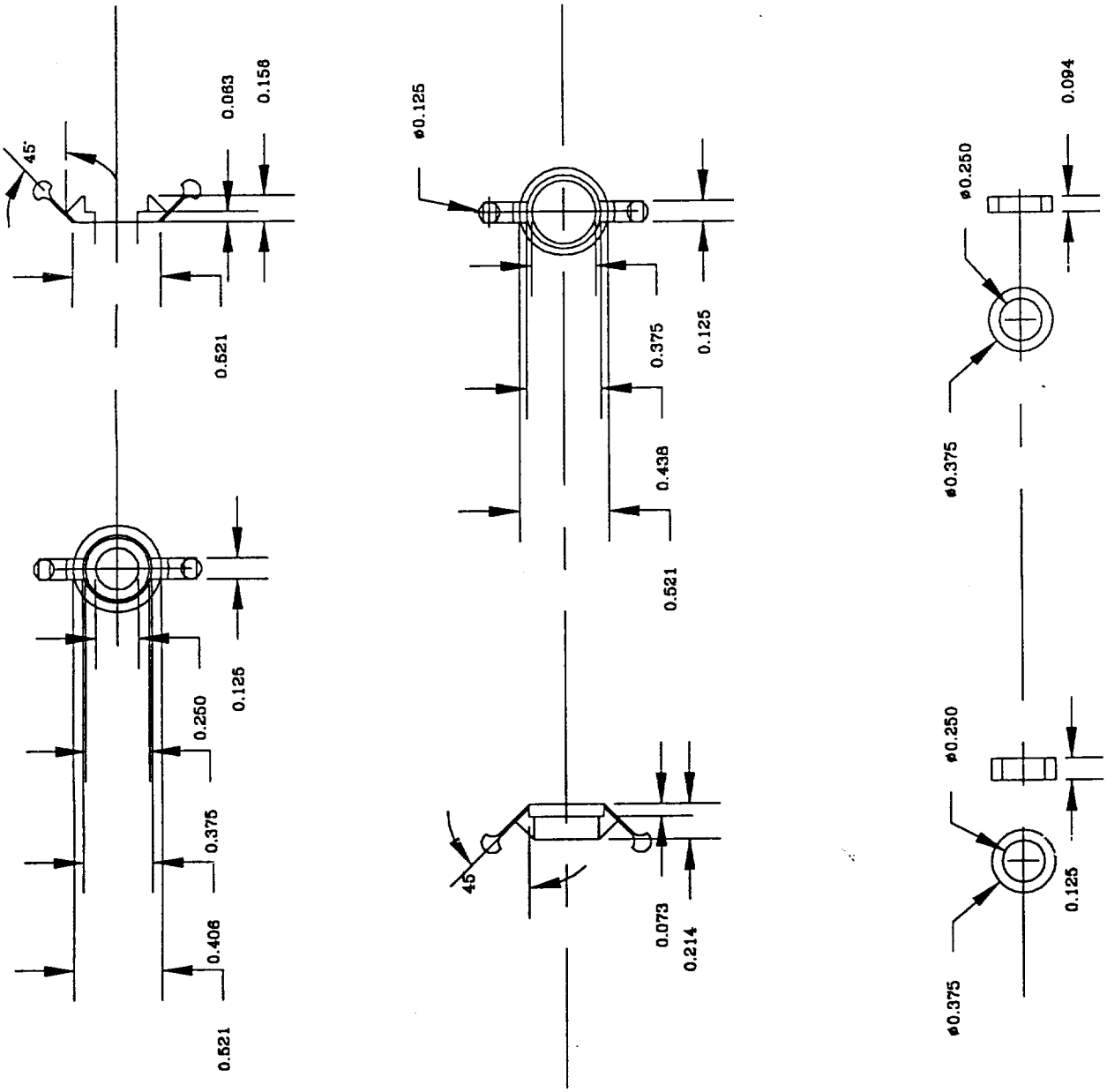
45°
0.083
0.158
0.521
0.125
0.250
0.375
0.406
0.521
ø0.125
0.125
0.375
0.438
0.521
45°
0.073
0.214
ø0.250
0.094
ø0.375
ø0.250
0.125
ø0.375

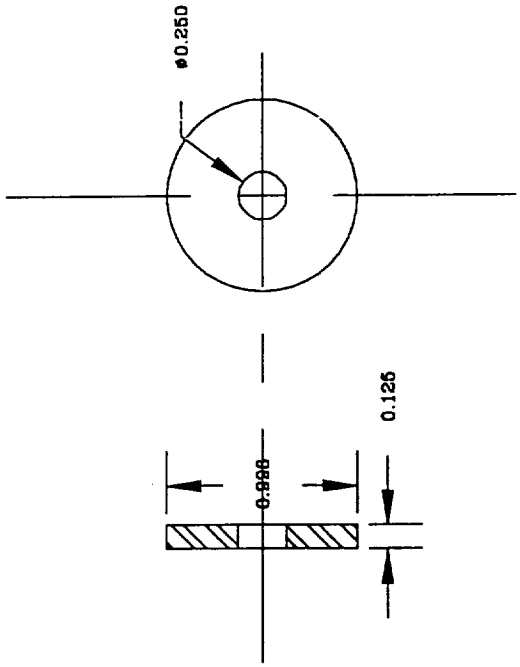
ø0.250
0.125
0.000

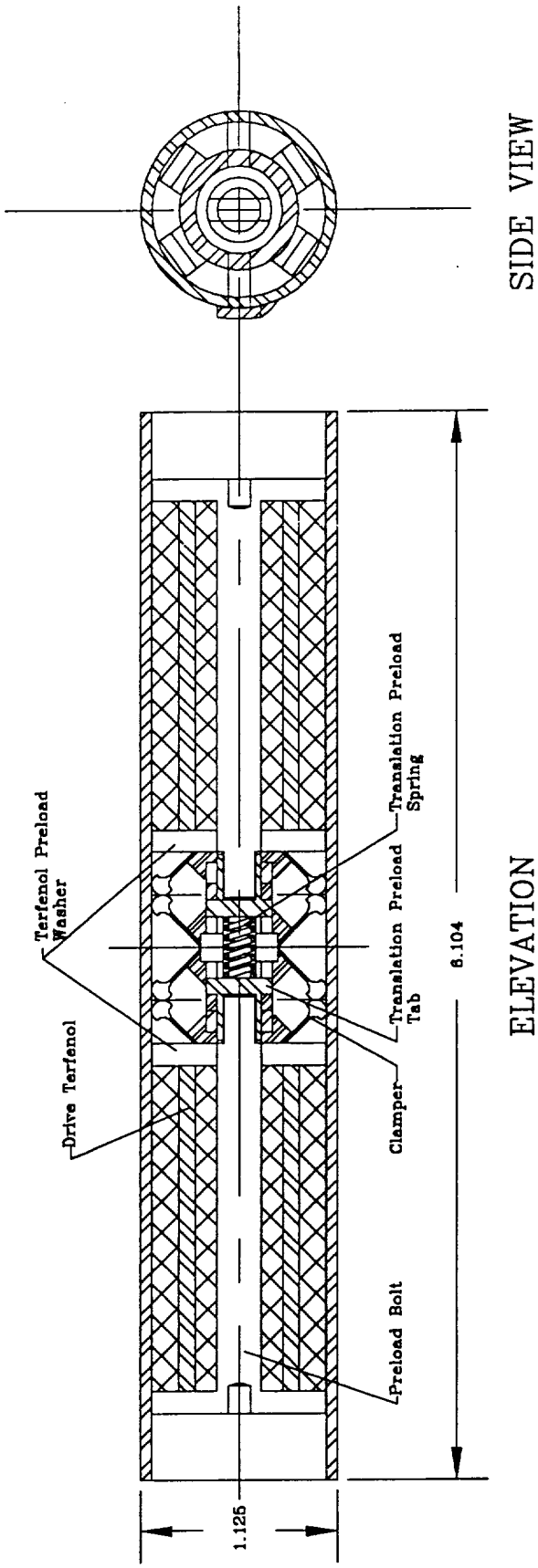
LINEAR ACTUATOR
SIDE VIEW
ELEVATION
Terfenol Preload Washer
Drive Terfenol
Translation Preload Spring
Translation Preload Tab
Clamper
Preload Bolt
6.104
1.125

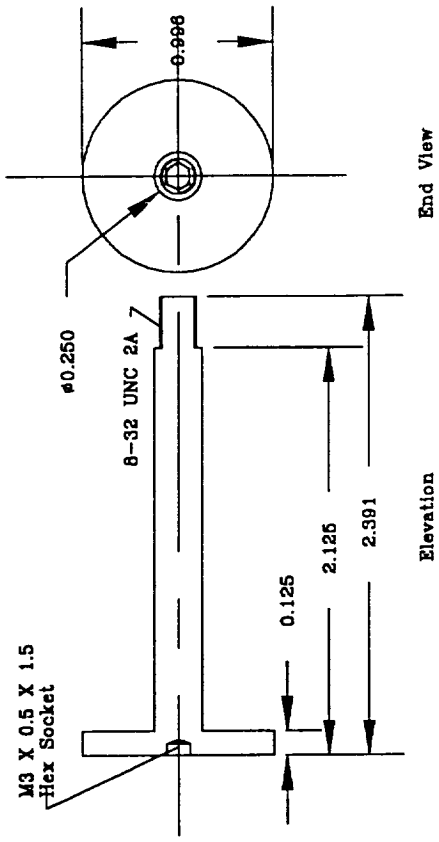
0.998
End View
ø0.250
8-32 UNC 2A
2.391
2.125
0.125
Elevation
M3 X 0.5 X 1.5
Hex Socket

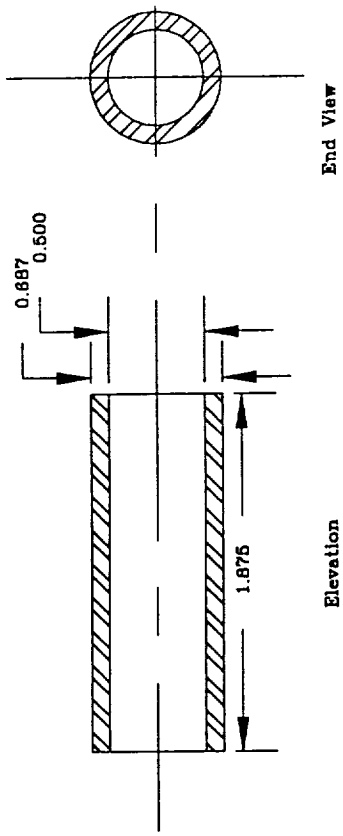
End View
0.687
0.500
1.875
Elevation

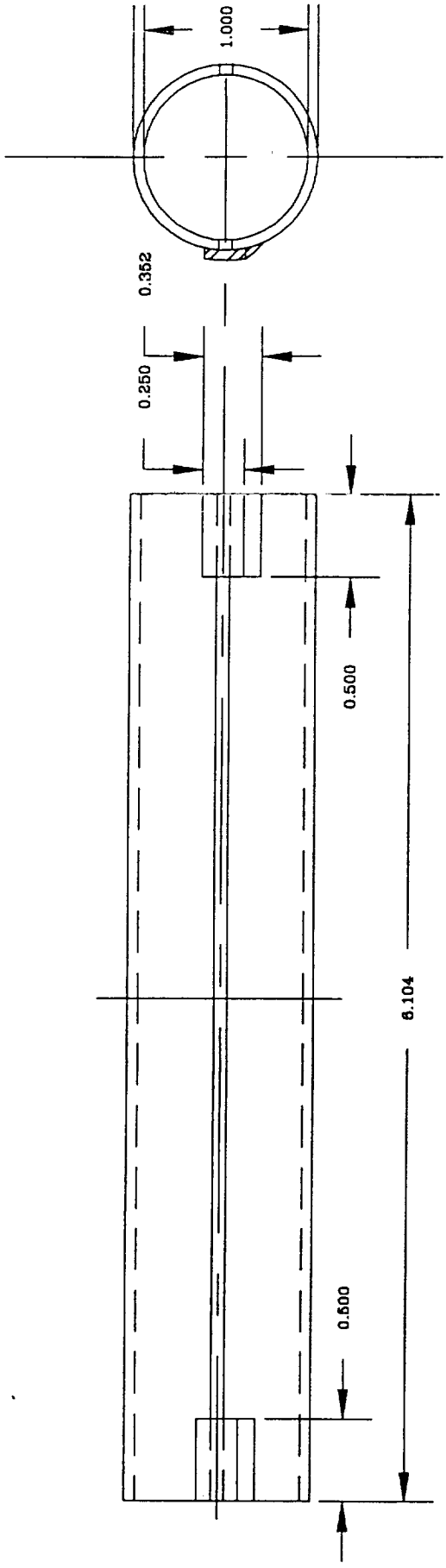

SIDE VIEW

ELEVATION

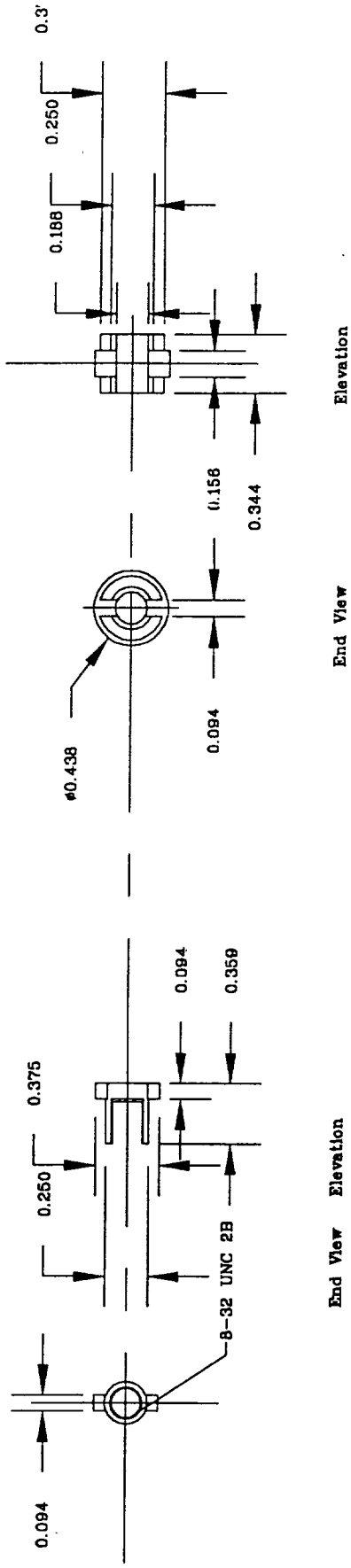
0.3
0.250
0.188
0.158
0.344
Elevation
ø0.438
0.094
End View
0.094
0.359
0.375
0.250
8-32 UNC 2B
End View
Elevation
0.094

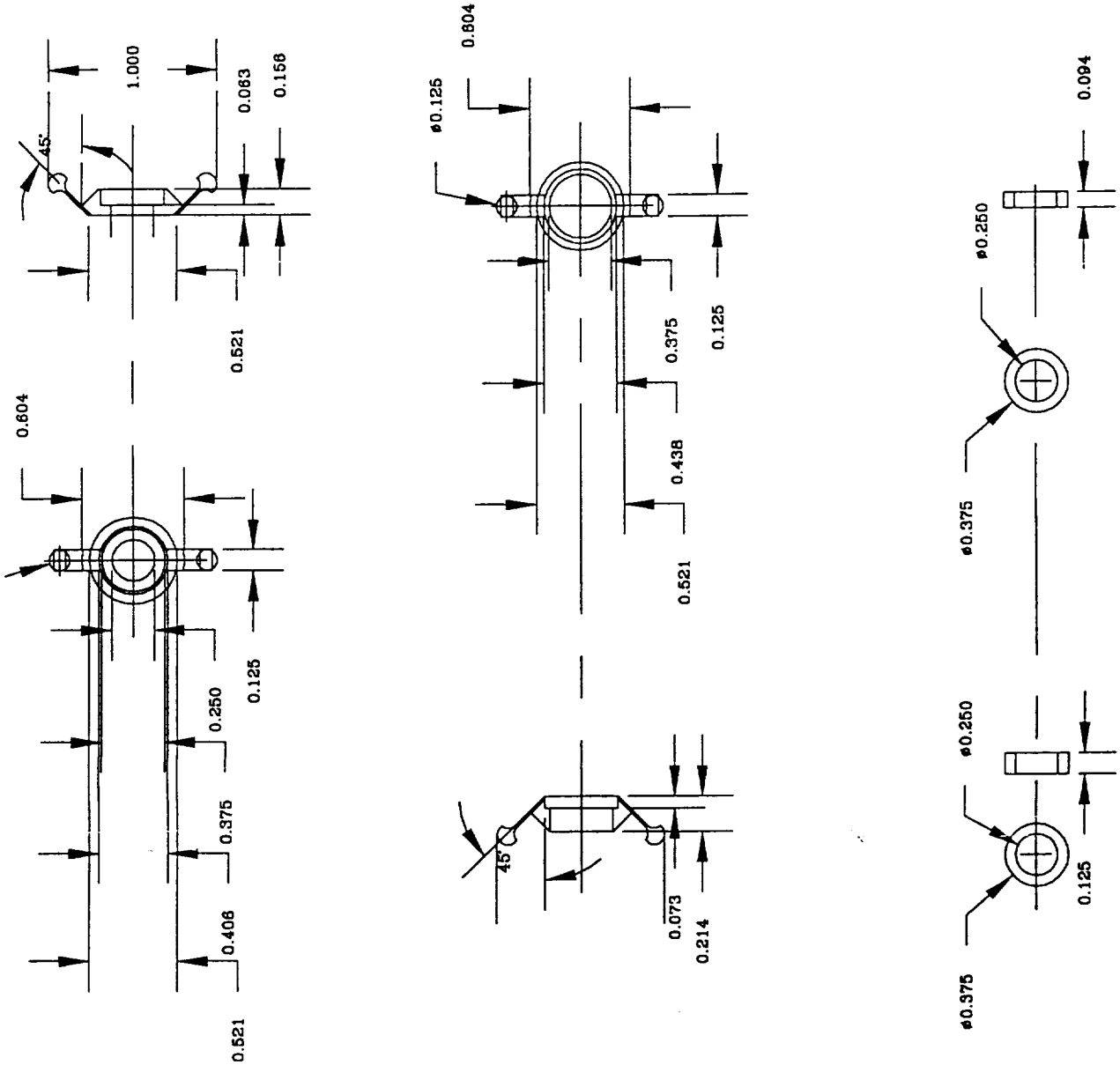
45°
1.000
0.063
0.156
0.521
0.604
0.125
0.250
0.375
0.406
0.521
0.604
ø0.125
0.375
0.125
0.438
0.521
45°
0.073
0.214
ø0.250
0.094
ø0.375
ø0.250
0.125
ø0.375

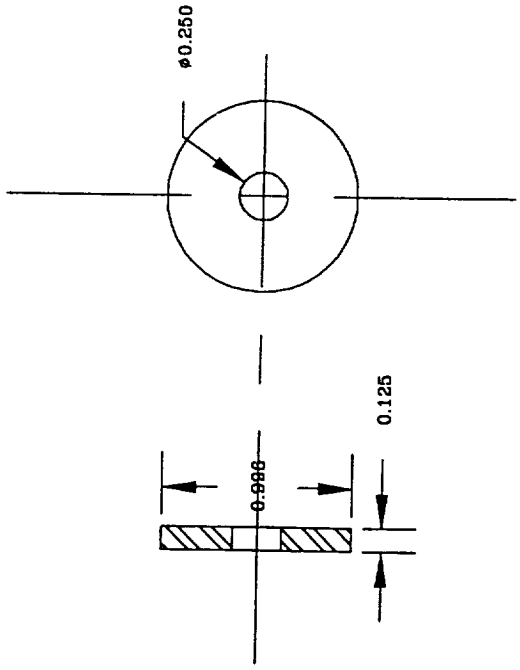
ø0.250
0.125
0.998